EXPERIMENTAL AND NUMERICAL INVESTIGATION ON PART THICKNESSES EFFECTS IN TAILOR WELDED BLANK PROCESS

ANAS BASRI BIN MUSTHAFA

UNIVERSITI MALAYSIA PAHANG

UNIVERSITI MALAYSIA PAHANG

BORANG PENGESAHAN STATUS TESIS ◆

JUDUL: EXPERIMENTAL AND NUMERICAL INVESTIGATION ON PART THICKNESSES EFFECTS IN TAILOR WELDED BLANK PROCESS

SESI PENGAJIAN: 2012/2013

Saya, **ANAS BASRI BIN MUSTHAFA (900809-06-5049)**
(HURUF BESAR)

mengaku membenarkan tesis (Sarjana Muda / ~~Sarjana / Doktor Falsafah~~)* ini disimpan di perpustakaan dengan syarat-syarat kegunaan seperti berikut:

1. Tesis ini adalah hakmilik Universiti Malaysia Pahang (UMP).
2. Perpustakaan dibenarkan membuat salinan untuk tujuan pengajian sahaja.
3. Perpustakaan dibenarkan membuat salinan tesis ini sebagai bahan pertukaran antara institusi pengajian tinggi.
4. **Sila tandakan (√)

[ ]	**SULIT**	(Mengandungi maklumat yang berdarjah keselamatan atau kepentingan Malaysia seperti yang termaktub di dalam AKTA RAHSIA RASMI 1972)
[ ]	**TERHAD**	(Mengandungi maklumat TERHAD yang telah ditentukan oleh organisasi / badan di mana penyelidikan dijalankan)
[√]	**TIDAK TERHAD**	

Disahkan oleh:

(TANDATANGAN PENULIS) (TANDATANGAN PENYELIA)

Alamat Tetap:

No. 51, JLN TJ 6/3
Taman Temerloh Jaya
28000 Temerloh
Pahang

DR. MOHD ZAIDI BIN SIDEK
(Nama Penyelia)

Tarikh: **27 JUN 2013** Tarikh: **27 JUN 2013**

CATATAN: * Potong yang tidak berkenaan.

** Jika tesis ini SULIT atau TERHAD, sila lampirkan surat daripada pihak berkuasa/organisasi berkenaan dengan menyatakan sekali tempoh tesis ini perlu dikelaskan sebagai SULIT atau TERHAD.

◆ Tesis dimaksudkan sebagai tesis bagi Ijazah Doktor Falsafah dan Sarjana secara Penyelidikan, atau disertasi bagi pengajian secara kerja kursus dan penyelidikan, atau Laporan Projek Sarjana Muda (PSM).

EXPERIMENTAL AND NUMERICAL INVESTIGATION ON PART THICKNESSES EFFECTS IN TAILOR WELDED BLANK PROCESS

ANAS BASRI BIN MUSTHAFA

Report submitted in partial fulfilment of the requirements
for the award of the degree of
Bachelor of Mechanical Engineering

Faculty of Mechanical Engineering
UNIVERSITI MALAYSIA PAHANG

JUNE 2013

EXAMINER'S DECLARATION

UNIVERSITI MALAYSIA PAHANG
FACULTY OF MECHANICAL ENGINEERING

I certify that the project entitled "*Experimental and Numerical Investigation on Part Thicknesses Effects in Tailor Welded Blank Process*" is written by Anas Basri Bin Musthafa. I have examined the final copy of this report and in my opinion, it is adequate in terms of language standard, and report formatting requirement for the award of the degree of Bachelor of Engineering. I herewith recommend that it be accepted in partial fulfillment of the requirements for the degree of Bachelor of Mechanical Engineering.

PM. Dr. Md. Mustafizur Rahman
Examiner

Signature

SUPERVISOR'S DECLARATION

I hereby declare that I have checked this project report and in my opinion this project is satisfactory in terms of scope and quality for the award of the degree of Bachelor of Mechanical Engineering.

Signature: 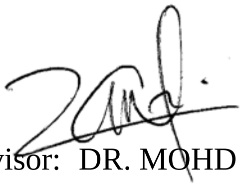

Name of Supervisor: DR. MOHD ZAIDI BIN SIDEK

Position: LECTURER

Date: 27 JUNE 2013

STUDENT'S DECLARATION

I hereby declare that the work in this report is my own except for quotations and summaries which have been duly acknowledged. The report has not been accepted for any degree and is not concurrently submitted for award of other degree.

Signature:

Name: ANAS BASRI BIN MUSTHAFA

ID Number: MA10090

Date: 27 JUNE 2013

ACKNOWLEDGEMENTS

All praise is to Allah with His Guidance and Benevolence; I had successfully accomplished my final year project. I am grateful and would like to express my sincere gratitude and appreciation to all those who gave me the possibility to complete this project. Special thanks is due to my supervisor, Dr. Mohd Zaidi Bin Sidek for his germinal ideas, invaluable guidance and whose help, stimulating suggestions and encouragement helped me in all time of this project.

I would also like to acknowledge with much appreciation the crucial role of the staff in Mechanical Laboratory, who gave me a permission to use the mechanical equipment and also the machine and giving a permission to use all the necessary tools in the laboratory.

My sincere thanks go to all lecturer and members of the staff of the Mechanical Engineering Department, UMP, who have given their full effort in guiding me in achieving the goal as well as their encouragement to maintain my progress in track. My profound thanks go to all classmates, especially to my friends for spending their time in helping and giving support whenever I need it in completing my project.

Not forgotten, I acknowledge my sincere indebtedness and gratitude to my parents for their love, dream and sacrifice throughout my life and consistently encouraged me to carry on my higher studies. I cannot find the appropriate words that could properly describe my appreciation for their devotion, support and faith in my ability to attain my goals. Thanks for all the support.

ABSTRACT

Tailor welded blank (TWB) is increasingly popular in producing sheet metal components especially for automotive industry. TWBs is employed by using dissimilar material welding which is mainly affected blank thickness and type of material used. This study is focused on the part thickness effects using experimental and numerical method. Thickness of tailor welded sheets plays an important role in sheet metal forming since fracture, wrinkling and weak spots are strongly influenced by material behaviour. In this study, simple heat transfer testing equipment is fabricated to conduct heat transfer experiment. A numerical and experimental study was carried out to investigate the heat transfer characteristic for different thickness of common used type of TWB material. The investigated thicknesses of aluminum 1100 are 1, 2 and 3 mm. Low heat capacity laser is used to measure the temperature distribution in experiment and used to validate FE model. A finite element model (2D) of aluminum 1100 is applied to simulate static heat distribution inside the material for different part thicknesses, heating position and amount of heat. The results shown that the heating region for thicker plate for combination 3 mm with 1 mm is 60 % wider compare to thinner plate with 40 %. Different combination of material thickness requires different heating positions and increasing the thickness of the material is increases the use of heat flux.

ABSTRAK

Tailor welded blank (TWB) semakin popular dalam menghasilkan komponen kepingan logam terutamanya bagi industri automotif. TWB telah digunakan dengan menggunakan kimpalan bahan yang berbeza yang mana sebahagian besarnya terjejas dengan ketebalan bahan dan jenis bahan yang digunakan. Kajian ini lebih tertumpu pada kesan ketebalan dengan menggunakan kaedah ujikaji dan kaedah berangka. Ketebalan pada kepingan *tailor* yang dikimpal memainkan peranan yang penting dalam membentuk kepingan logam sementara kepatahan, kedutan dan kawasan lemah adalah dipengaruhi oleh kelakuan bahan. Dalam kajian ini, satu peralatan untuk menjalankan eksperimen pemindahan haba telah dicipta. Satu eksperimen dan kajian berangka telah dijalankan untuk menyiasat ciri-ciri pemindahan haba bagi ketebalan yang berbeza dari jenis bahan TWB yang biasa digunakan. Ketebalan aluminium jenis 1100 yang dikaji adalah 1, 2 dan 3 mm. Laser dengan muatan haba yang rendah digunakan untuk mengukur taburan suhu dalam eksperimen dan digunakan untuk mengesahkan FE model. Satu model (2D) *finite element* dengan material aluminium jenis 1100 digunakan untuk mensimulasikan pengagihan haba statik dalam bahan untuk bahagian ketebalan yang berbeza, posisi pemanasan dan jumlah haba. Keputusan menunjukkan bahawa kawasan pemanasan untuk plat yang tebal bagi kombinasi 3 mm dengan 1 mm adalah 60 % lebih luas berbanding dengan plat yang nipis dengan 40 %. Kombinasi ketebalan bahan yang berbeza memerlukan posisi pemanasan yang berbeza dan bertambahnya ketebalan bahan ini akan meningkatkan penggunaan fluks haba.

TABLE OF CONTENTS

		Page
EXAMINER'S DECLARATION		ii
SUPERVISOR'S DECLARATION		iii
STUDENT'S DECLARATION		iv
ACKNOWLEDGEMENTS		v
ABSTRACT		vi
ABSTRAK		vii
TABLE OF CONTENTS		viii
LIST OF TABLES		x
LIST OF FIGURES		xi
LIST OF ABBREVIATIONS		xiii
CHAPTER 1	**INTRODUCTION**	1
	1.1 Overview Project	1
	1.2 Computer Aided Engineering	3
	1.3 Problem Statement	5
	1.4 Objectives of the Study	5
	1.5 Scopes of the Study	5
	1.6 Outline of Report	6
CHAPTER 2	**LITERATURE REVIEW**	7
	2.1 Introduction	7
	2.2 Tailor Welded Blanks	7
	2.3 Welding	11
	2.3.1 Laser and Mash Seam Welding	12
	2.4 Heat Affected Zone	15
	2.5 Thermocouple	17
	2.6 Material Properties	18

CHAPTER 3 METHODOLOGY 20

3.1 Introduction 20
3.2 Project Flow Chart 20
3.3 Test Rig 22
3.3.1 Fabrication process 23
3.3.2 Experimental setup 25
3.3.3 Experimental Procedure 29
3.4 Simulation Setup 30

CHAPTER 4 RESULTS AND DISCUSSION 33

4.1 Introduction 33
4.2 Test Rig Fabrication 33
4.3 Heat Transfer Analysis 34
4.3.1 Comparison of Experimental and Simulation 35
4.4 Parametric Study 38
4.4.1 Optimum Parameter 41

CHAPTER 5 CONCLUSIONS AND RECOMMENDATIONS 43

5.1 Introduction 43
5.2 Conclusions 43
5.3 Recommendations and Further Research 44

REFERENCES 45

APPENDICES 48

A Parts Drawing 49
B Simulation Figures 51
C1 Parametric Study on Thickness of 3 mm and 1 mm 53
C2 Parametric Study on Thickness of 3 mm and 2 mm 55
C3 Parametric Study on Thickness of 2 mm and 1 mm 57

LIST OF TABLES

Table No.	Title	Page
2.1	Material properties at room temperature	19
3.1	Bill of material test rig	23
3.2	Thickness combinations of specimens for each case	26
3.3	Laser welding parameters	29
3.4	Thermal properties of aluminium material	31
3.5	Parametric of heat source	32
4.1	Maximum temperature from experimental and simulation for thickness 3 mm with 1 mm	35
4.2	Maximum temperature from experimental and simulation for thickness 3 mm with 2 mm	36
4.3	Maximum temperature from experimental and simulation for thickness 2 mm with 1 mm	37
4.4	Optimum parameters	42

LIST OF FIGURES

Figure No.	Title	Page
2.1	Exploded view of current and potential automotive tailor welded blank applications	9
2.2	Typical parts made of tailored blanks	10
2.3	B-Pillar of a late model BMW X5	10
2.4	Post-weld processing of TWB	12
2.5	Laser and mesh seam welding	13
2.6	Comparison of conduction and keyhole welding	15
2.7	Schematic of heat affected zone	16
2.8	Schematic drawing of a thermocouple	17
3.1	Project flow chart	21
3.2	Drawing of test rig	22
3.3	Assembly part of test rig	23
3.4	(a) Conventional milling machine, (b) CNC milling machine	24
3.5	Fabrication process	25
3.6	Schematic of experimental layout	26
3.7	Specimen test (Aluminum 1100 material)	26
3.8	Drilling process using EDM super drilling machine	27
3.9	Position of points on the specimen	27
3.10	Measuring tools component	28
3.11	Experimental apparatus	29
3.12	Position of heat source on specimen model for simulation	31
3.13	Position of heat imposed on modeling specimen for parametric study	31

4.1	(a) Test rig, (b) Specimens material was clamped on the test rig	34
4.2	Comparison result for thickness 3 mm with 1 mm	35
4.3	Comparison result for thickness 3 mm with 2 mm	36
4.4	Comparison result for thickness 2 mm with 1 mm	37
4.5	Temperature distribution for different position of heating and heat flux on thickness 3 mm with 1 mm	39
4.6	Temperature distribution for different position of heating and heat flux on thickness 3 mm with 2 mm	40
4.7	Temperature distribution for different position of heating and heat flux on thickness 2 mm with 1 mm	41
A.1	Base part	49
A.2	Base leg part	49
A.3	Stopper part	50
A.4	Clamper part	50
B.1	Thickness 3 mm with 1 mm	51
B.2	Thickness 3 mm with 2 mm	51
B.3	Thickness 2 mm with 1 mm	52
C.1	Different heating position with 54×10^6 W/m^2 of heat flux	53
C.2	Different heating position with 62×10^6 W/m^2 of heat flux	55
C.3	Different heating position with 51×10^6 W/m^2 of heat flux	57

LIST OF ABBREVIATIONS

1D	One dimensional
2D	Two dimensional
3D	Three dimensional
BMW	Bayerische Motoren Werke
CAE	Computer Aided Engineering
CFD	Computational Fluid Dynamics
CNC	Computer Numerical Control
CO_2	Carbon dioxide
EDM	Electrical discharge machining
FE	Finite element
FEA	Finite element analysis
FEM	Finite element method
FYP	Final year project
FZ	Fusion zone
HAZ	Heat affected zone
LBW	Laser beam welding

CHAPTER 1

INTRODUCTION

1.1 OVERVIEW PROJECT

Sheet metal forming has a very important role in the manufacturing of complex automotive and other sheet metal components in a manner which minimizes waste material and energy utilization and permits the designer to use the intrinsic properties of the material. (Panda et al., 2007). The automotive and aeronautic industries are working continually to develop and apply technology that reduces the cost and weight of their products, thus minimizing the energy consumption and environmental impact of future products. Vehicle and aircraft weight reduction through the use of advanced materials and manufacturing methods is of interest to all major manufacturers. Automotive engineers have also been successful in reducing weight, part counts, and cost and in streamlining the assembly process through the use of steel tailor welded blanks (TWBs) to replace multiple blanks that have to be stamped separately and then assembled. (Davies et al., 2002).

Tailor welded blanks are defined as two or more separate pieces of flat material, dissimilar thickness, and/or mechanical properties, jointed together before forming to provide customized and superior qualities in the finished stamping. The traditional procedure in the automobile industry was to stamp the automobile parts with different thickness and different materials one by one, and then these stamped parts were welded together to form one piece of complete automobile part. With the application of tailor welded blank, the combination of different thickness and different materials is formed first by laser welding, then tailor welded blank is stamped into one piece of complete automobile part. (Qi, 2012).

According to Qi (2012), by utilizing a tailor welded blank, made up of blanks of different thickness, coatings, and/or strength, the final stamped part can exhibit specific desired properties. Tailor welded blanks can yield several benefits such as:

(i) Reduction of final car weight.

- The use of different strength or thickness in a single part can simplify the whole structure of a vehicle. It will reduce fuel consumption that is very important for energy saving.
- Example; in an automotive application, the TWB eliminate need for reinforcement, resulting in an overall reduction in vehicle body weight.

(ii) Reduction of automobile parts' number.

- The precision of car body structure can be improved and a lot of press equipment and working procedures can be saved.
- By using a tailor welded blank with a large, thin, soft piece of material jointed to a smaller, thicker, stronger piece of material, the blank can be formed and used as a one piece door inner, thus completely eliminating the previous reinforcing components.

(iii) Improved raw material utilization and reduction of scrap.

- By using higher strength and heavier gauge materials to the specific areas, the reduction in material could be realized.

(iv) Improvement on the functional performance.

- The structural rigidity can be improved due to possibility by optimizing selection of material based on appropriate strength or gauge.

(v) Potential to produce wide width automobiles.

- Automobile industry shows great concern on the wide width steel sheets while the width of steel sheets is constrained by the roller machine. Tailor welded blanks can solve this problem. At present, supply of the steel with wide width cannot meet the large demand of the market. Tailor welded blanks provide this solution.

.

Within the automotive body-in-white structural parts, more and more typical parts such as rail, door inner, bumper, side ring, and reinforcement had used the tailor welded blanks before stamping process. At present, two or three automotive parts using tailor welded blanks in the present car design. For the expensive cars, tailor welded blanks is the better choices in car design. By using tailor welded blanks, the overall anti-crash performance of the vehicle is improved. New applications for tailor welded blanks continue to increase because car designers and manufactures believe the using of tailor welded blanks in the automotive structural parts can simplify the manufacturing process, reduce the cost of production, and improve the overall quality of the vehicle. (Qi, 2012).

1.2 COMPUTER AIDED ENGINEERING

Computer-aided engineering (CAE) is the use of computer software to assist in the resolution of engineering design for a wide range of industries. This includes simulation, validation, and optimization of products, processes, and manufacturing tools. A typical CAE process comprises of pre-processing, solving, and post-processing steps. In the pre-processing phase, engineers model the geometry and the physical properties of the design, as well as the environment in the form of applied loads or constraints. Next, the model is solved using an appropriate mathematical formulation of the underlying physics. In the post-processing phase, the results are presented to the engineer for review. (Siemens, 2013a). CAE applications support a wide range of engineering disciplines or phenomena including:

- Stress and dynamics analysis on components and assemblies using finite element analysis (FEA).
- Thermal and fluid analysis using computational fluid dynamics (CFD).
- Kinematics and dynamic analysis of mechanisms (multibody dynamics).
- Mechanical event simulation (MES).
- Control systems analysis and optimization of the product or process.
- Simulation of manufacturing processes like casting, moulding and die press forming.

Finite element analysis (FEA) is the modeling study of products and systems in a virtual environment, for the purpose of finding and solving potential (or existing) structural or performance issues. FEA is the practical application of the finite element method (FEM), which is used by engineers and scientist to mathematically model and numerically solve very complex structural, fluid, and multiphysics problems. FEA software can be utilized in a wide range of industries, but is most commonly used in the aeronautical, biomechanical and automotive industries. A finite element (FE) model comprises a system of points, called “nodes”, which form the shape of the design. Connected to these nodes are the finite elements themselves which form the finite element mesh and contain the material and structural properties of the model, defining how it will react to certain conditions. The density of the finite element mesh may vary throughout the material, depending on the anticipated change in stress levels of a particular area. Regions that experience high changes in stress usually require a higher mesh density than those that experience little or no stress variation. Points of interest may include fracture points of previously tested material, fillets, corners, complex detail, and high-stress areas. (Siemens, 2013b).

FE models can be created using one-dimensional (1D beam), two-dimensional (2D shell) or three-dimensional (3D solid) elements. By using beams and shells instead of solid elements, a representative model can be created using fewer nodes without compromising accuracy. Each modeling scheme requires a different range of properties to be defined, such as section areas, moments of inertia, torsional constant, plate thickness, bending stiffness, transverse shear, etc. (Siemens, 2013b). To simulate the effects of real-world working environments in FEA, various load types can be applied to the FE model, including:

- Nodal: forces, moments, displacements, velocities, accelerations, temperature and heat flux
- Elemental: distributed loading, pressure, temperature and heat flux
- Acceleration body loads (gravity)

Heat is major parameters in TWB process. Hence, it must be optimized for the process. Among the considered factors are to minimize heating width and use high intensity heat flux to generate enough heating energy inside the work-piece. This study is concentrate heat transfer characteristic for the common used type of TWB material with different thickness. Actual heat distribution will be measured in experiment and will be used to validate FE model. Finally, FE model will develop for joining two different part thickness using TWB process. And to simplify this study will consider for the case of unmoved heat source.

1.3 PROBLEM STATEMANT

Tailor-welded blanks provide numerous benefits including reduced vehicle weight, lower manufacturing costs, and improved structural integrity. However, employing TWBs is the inhomogeneity of the blanks due to the material and weldment, which can affect the formability of the TWBs. Thickness of tailor welded sheets plays an important role in sheet metal forming since fracture, wrinkling and weak spots are strongly influenced by material behaviour. This research is investigating heat transfer characteristic for the different thickness of common used type of TWB material.

1.4 OBJECTIVES OF THE STUDY

The objectives of this research are stated below:

(i) To fabricate test rig for heat transfer experiment and conduct the experiment test.
(ii) To compare the result of experimental test with simulation heat transfer modeling.
(iii) To study parametric using FE analysis to investigate TWB process.

1.5 SCOPES OF THE STUDY

This research is focus on method joining of automotive panels which is to investigate the heat transfer through the joining on similar material with different thickness. This study has been conducted based on the following scopes:

(i) Design and machining simple test rig.
(ii) Analysis on specimen test of aluminum material but different thickness.

(iii) Perform heat transfer tests (using localised heating condition on each material thickness).

(iv) Develop finite element (FE) 2D model to simulate heat distribution inside the metal.

(v) Study the heating position on material with different thickness and amount of heat flux for TWB process.

1.6 OUTLINE OF REPORT

Chapter 1 introduces the overview of project, computer aided engineering, problem statement, the objectives of this study and the scopes of this study. Chapter 2 presents the literature study about Tailor Welded Blank, welding process, thermocouple and material properties used. Chapter 3 discusses the methodology from designing until how to run the experiment, finite element modeling and the optimization parameter. Chapter 4 discusses the results and analysis of the heat transfer analysis with comparison of experimental result and simulation result. It also discusses the optimization of heat source parameters using FE analysis. Chapter 5 presents the conclusion and recommendation of the future research.

CHAPTER 2

LITERATURE REVIEW

2.1 INTRODUCTION

This chapter discusses about the research of the Tailor Welded Blank parts and explained about welding process for TWB. It also covers on an application of different material thickness in TWB.

2.2 TAILOR WELDED BLANKS

The automotive industry is an extremely competitive global market that is continuously challenged to improve its products and operations. Customers demand high performance cars at minimal cost, which often conflict with the ever constricting government environmental regulations. These requirements force automakers to come up with innovative solutions to reduce manufacturing costs, improve product performance, and reduce vehicle weight. (Kinsey et al., 2000).

Recently, the automobile industries have tried to develop various types of cars with high quality and low cost to meet customers’ demands. As a new way to achieve this goal, welding methods such as laser welding and the mash seam welding process were introduced for structural frames. These sheets are called tailor-welded blanks (TWBs) for presswork production. These types of blanks have several advantages in the manufacturing of automobiles: low cost, less scrap, reduction of car weight, and flexibility for component design in mass production. (Mallieswaran et al., 2012).

Especially, using the laser welding process, high strength, high hardness of the welded zone and a narrow heat-affected zone can make it possible to manufacture superior parts. (Heo et al., 2001). With TWBs, welding occurs prior to, rather than after, the stamping process. A typical TWB is laser welded and comprised of two or more sheets. Each sheet typically has a different thickness, although sheets with different strengths, formability's and/or coatings are also common. (Clapham et al., 2004).

Tailor Welded Blanks (TWB) are blanks composed of sheets of dissimilar or similar thicknesses, strength or coatings etc. welded in a single plane before forming. (Pallet and Lark, 2001). In terms of applications, TWBs were first used to overcome design challenges with the available material, such as the floor plate of the Audi 100 (Rooks, 2001). The floor plate of the Audi design specification was greater than the width of the steel supplied and thus, two sheets of steels were welded together to create the TWB. Other applications of TWBs have been in structural members where different thicknesses of steels were welded together such as for center pillars as commonly used in North America (Auto/Steel Partnership, 1995). Currently most chassis/body structural members are being made as TWBs.

Figure 2.1 shows examples where TWBs can be found in a vehicle. These TWBs consist of different grades and/or thicknesses of steel welded together to form optimized blanks that take advantage of the localized materials properties. For example:

a) Using thicker material near the engine fire wall and hinge area improves the crash performance, and
b) Using thinner material near the rear to reduce weight (Auto/Steel Partnership, 1995); thereby, reducing the overall weight of the vehicle.

Therefore, it is expected that the number of TWBs in automotive parts manufacturing will increase with the improvement in welding technology and development of newer light materials available. TWBs began appearing in Europe and Japan in the mid-1980s, and their use has continued to increase. It is estimated that 40 to 60 million TWBs will be produced in 2000. (Das, 2000).

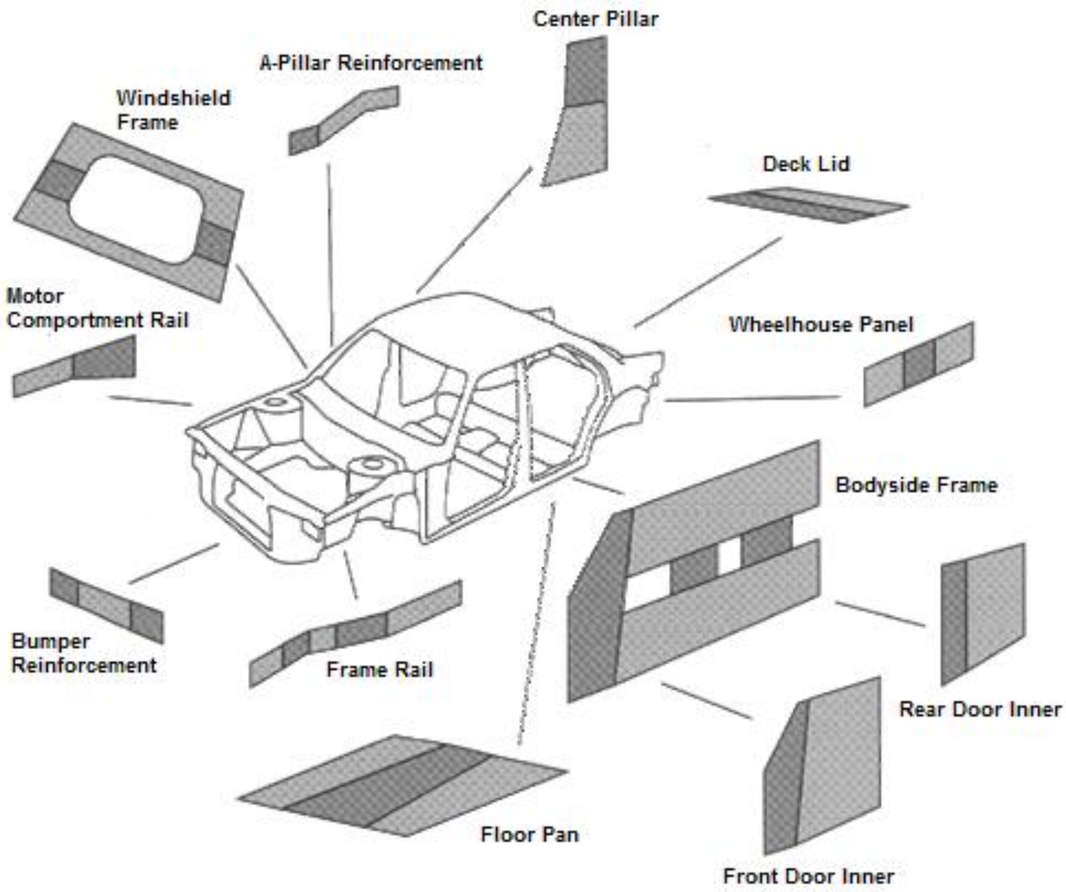

Figure 2.1: Exploded view of current and potential automotive tailor welded blank applications

Source: Auto/Steel Partnership (1995)

Aluminum alloys have been widely used in different industrial applications such as tanks, pressure vessels, aerospace, and vehicles because of their high specific strength, heat conductivity, and good properties at low temperatures. The use of aluminum alloys within sheet metal processing particularly in the automotive and transportation sectors is increasing with the continuing drive to reduced weight and improved efficiency. (Brown et al., 1995). Any combination of steel material or thickness can be used to manufacture a tailored blank by laser; possible limits to the application arise only as a result of the subsequent processing periods during forming. Figure 2.2 shows the illustrations of different tailored blanks give some idea of the possibilities offered today by laser and mash-seam welding techniques.

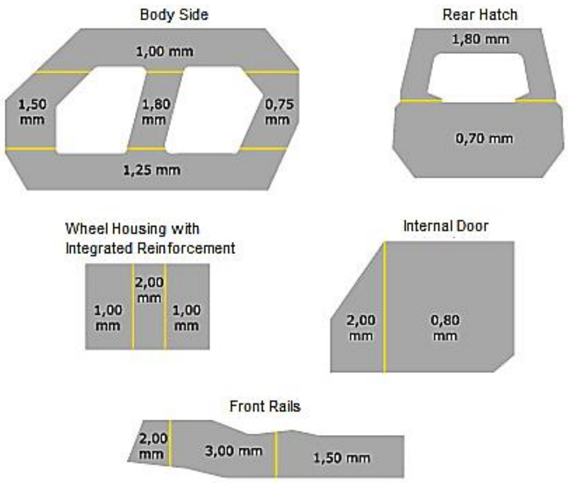

Figure 2.2: Typical parts made of tailored blanks

Source: TTB (2012)

For example, the B-pillar is made from tailored rolled steel blanks that allow parts to have different thicknesses through one part. The 2013Ford Focus has made the B-pillar part with eight thicknesses on the Focus B-pillar range from a maximum of 2.7 mm to as thin as 1.35 mm. The BMW automobiles also had made B-pillar part from Ultra High Strength Steel (UHSS) material with varies thickness as shown in Figure 2.3. (Smith, 2012).

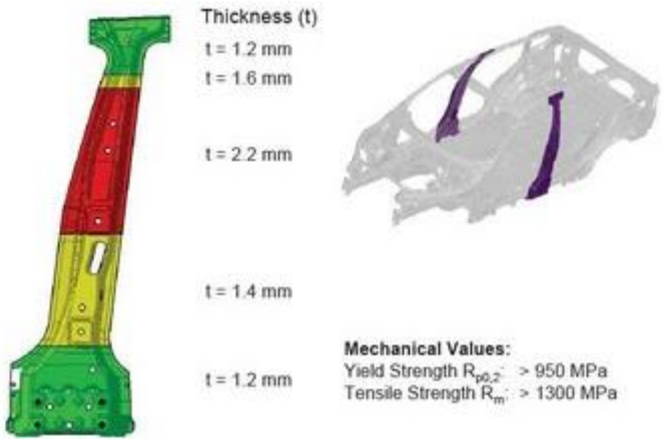

Figure 2.3: B-Pillar of a late model BMW X5

Source: Smith (2012)

2.3 WELDING

Joining of two dissimilar materials has been given more attention in recent years because of their superior capabilities. The example of the combination two dissimilar materials is the combination between aluminum and steel due to their potential in automotive applications. Suitable welding process and the welding technique is a significant consideration in tailor welded blank process. For example, joining of aluminums and steel should be made through some advance welding technique and welding process due to the melting temperature between these two materials are quite different. (Padmanabhan et al., 2006). The various welding process differ considerably in terms of temperature and pressure are combined and achieved. They also vary as to the attention that must be given to the cleanliness of the metal surfaces prior to welding and to possible oxidation or contamination of the metal during welding. If high temperature is used, most metal are affected more adversely by surrounding environment. (Garmo, 1974).

A tailor welded blank is comprised of two or more sheets that have been welded together in a single plane previous to forming. The sheets can be identical, or they can have different thickness, mechanical properties or surface coatings. They can be joined by various welding processes. For example, laser welding, mash seam welding, electron-beam welding and induction welding. (Saunders and Wagoner, 1995). Figure 2.4 shows the TWB part's post-weld processing.

Tailor welded blanks consist of two or more steel sheets of varying properties which are tailored into patterns that enable the required properties to be located precisely where they are needed within the final part. Because the production of tailor welded blanks relies on the fusion process, most traditional welding methods can be used to produce tailor welded blanks. Each welding method has certain characters that will generate different results such as finished blank appearance, formability, welding speed, flexibility and capital input, etc. (Qi, 2012). But most common methods to produce tailor welded blanks at present situation are laser welding and mash seam welding because the low heat input applied by these methods does not cause too much thermal distortion.

Figure 2.4: Post-weld processing of TWB

Source: Saunders and Wagoner (1995)

2.3.1 Laser and Mash Seam Welding

To create a Tailored Blank two or more sheets are welded together. This can be done by various welding processes, of which mash seam welding and laser welding are the commonly used processes, see Figure 2.5. The overlap of the parts to be joined is approximately 1-2 times the average sheet thickness in mash seam welding. (Bouaifi and Sommer, 1997). Tailored blanks are usually produced by laser welding. Due to small size of the weld cross-section it is not possible to use standard tests to determine mechanical properties of the weld zone in tailor-welded blanks. (Rojek et al., 2012). Laser welding technique has been widely used in the automotive industry. Nd: YAG lasers or CO_2 lasers are frequently used in the continuous or pulsed mode to act as heating sources. There are two types of welding mode: conduction welding and penetration welding. The conduction welding mode is applied for micro joining process, and the penetration welding allows for much higher ratio of depth to width. (Karagiannis and Chryssolouris, 2003).

Both weld types have their own characteristics. The width of a mash seam weld including the heat affected zone is 10-15 mm; the width of a laser weld including the heat affected zone is 1-2 mm. (Saunders and Wagoner, 1996). The volume fraction of martensite in the laser weld is large due to the high temperature rates during the cooling of the laser weld. Due to the lower temperature rates in mash seam welding, less martensite is formed, and consequently a less hard weld is formed.

As a result the mash seam weld can have a better formability than the laser weld. A disadvantage of the mash seam weld is its visibility in contrast to the almost invisible laser weld. Therefore mash seam welded Tailored Blanks will not be used in visible parts of a car. An advantage of laser welding is the narrow weld which hardly effects the cathodic protection in galvanised Tailored Blanks. (Meinders et al., 1998). According to Li (2010), the differences between laser welding and mash welding are as follows:

a) Laser welding is a fusion-welding process, which joins the materials by localized melting by using a laser beam. The fusion zone (FZ) and heat-affected zone (HAZ) are narrow due to low heat input; and
b) Mash welding is a fusion-welding process that bonds two pieces of overlapping materials together through diffusion when passing through rollers under a high load.

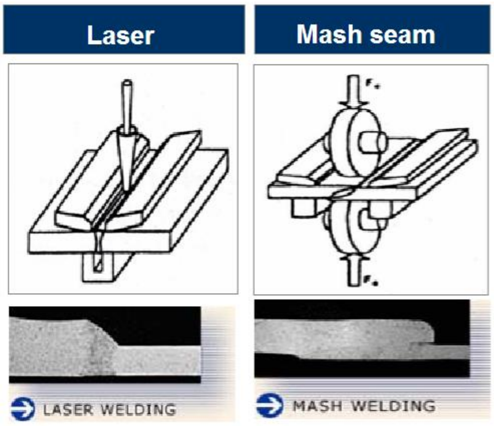

(a) Schematic welding process

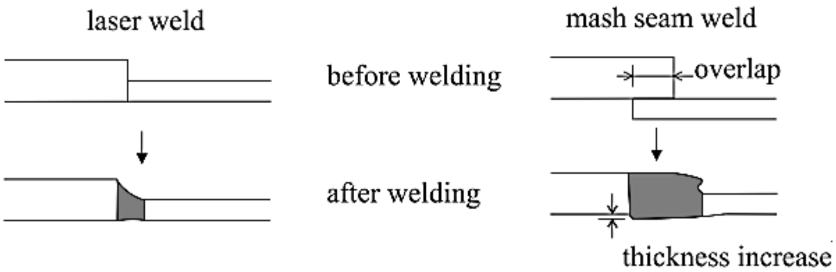

(b) Welding condition

Figure 2.5: Laser and mesh seam welding

Source: Li (2010)

Welds produced with lasers are preferred in many instances over other methods due to its appearance quality and internal quality. In addition, the economic advantage using laser welding is apparent because sound welded joints are being produced at rapid, competitive welding speeds. Today, lasers touch many aspects of our lives, even in the compact disc player we had in our daily life. The real evidence of success in the world using laser welded blanks indicates the choosing of laser welding as for the production methods of tailor welded blanks will be superior in nearly every application. (Qi, 2012).

The word LASER stands for “Light Amplification by Stimulated Emission of Radiation”. By the amplification of light in a resonator, a beam of coherent light with a high energy density was generated. This laser beam can be used in a lot of different ways like cutting, heat treatment, measuring, and welding. Recently, Laser welding, also known as Laser Beam Welding (LBW) has started to achieve a more widespread usage even it is a relatively new welding process that’s been around for a few decades ago. Initially it was used for exotic metal types that were hard to weld by conventional welding processes. But as time and technology grown, laser welding has moved into a more prominent position amongst the various types of welding processes. Huntington and Eagar studied laser light absorption on aluminum and aluminum alloys. Laser welding of aluminum alloys has been applied in various industrial applications. (Huntington and Eager, 1982).

Lasers are available in sizes up to 25 kW power output. Lasers in the size range 3 kW to 10 kW are usually adequate for the aluminum sheet thicknesses automotive applications. Laser welding aluminum alloys offers many advantages such as narrow heat-affected zone, narrow weld bead, precise heat input, minimal thermal distortion, as well as elevated welding speeds on thin sections and deep penetration on thick sections. Because of these advantages, the application of laser welding of aluminum alloys is increasing in the automobile sector for body and exterior panelling. (KM, 2009).

In laser welding, a laser beam is focused on a workpiece where the absorption of the radiation leads to a local heating and fusion of the workpiece. In general, there are two different basic methods that should be distinguished: conduction welding and keyhole or penetration welding. The main difference between these modes is that the surface of the weld pool remains unbroken for the conduction welding process, i.e., the laser radiation does not penetrate into the material being welded. As a result, conduction welds are less susceptible to gas entrapment during the welding process. In keyhole welding, when the laser intensity is higher than approximately 10^6 W/cm^2 the weld pool opens and forms a narrow slot or keyhole so that the laser beam can enter the weld pool. The result is that the laser beam not only melts, but also evaporates the material. (Thasanaraphan, 2012). The schematic sketches of these two welding modes are shown in Figure 2.6.

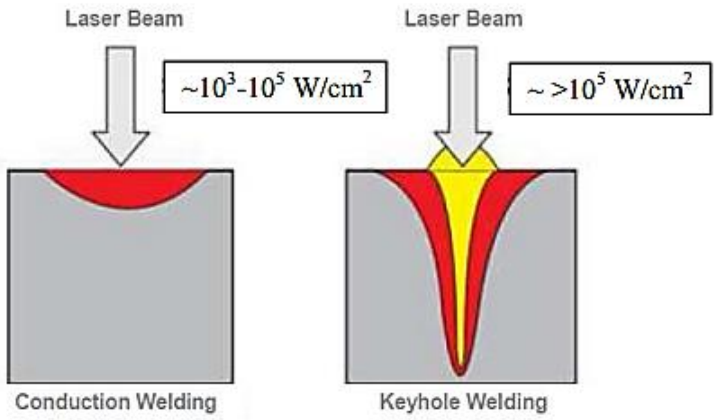

Figure 2.6: Comparison of conduction and keyhole welding

Source: Schuöcker (1998)

The typical spot sizes in industrial laser welding usually range from about 0.1 to 1.0 mm, with 0.3 mm being a common size. For the overlapping welds the laser spot size is usually set to about the desired weld width. (Migliore, 1998).

2.4 HEAT AFFECTED ZONE

The heat affected zone is typically defined as the area of base material, either a metal or a thermoplastic, which has had its microstructure and material properties have been altered by the welding process and subsequent re-cooling or heat intensive cutting operations. (Grande et al., 2012).

The heat from the welding process and subsequent re-cooling causes this change from the weld interface to the termination of the sensitizing temperature in the base metal. The extent and magnitude of property change depends primarily on the base material, the weld filler metal, and the amount and concentration of heat input by the welding process. (Weman, 2003). The thermal diffusivity of the base material plays a large role. If the diffusivity is high, the material cooling rate is high and the HAZ is relatively small. Alternatively, a low diffusivity leads to slower cooling and a larger HAZ. The amount of heat inputted by the welding process plays an important role as well, as processes like oxyfuel welding use high heat input and increase the size of the HAZ. Processes like laser beam welding and electron beam welding give a highly concentrated, limited amount of heat, resulting in a small HAZ. (Weman, 2003).

Figure 2.7 shows the schematic of heat affected zone. The size of the heat affected zone is a function of the laser pulse duration and the material parameters such as specific heat and thermal conductivity. The heat affected zone will depend on the distance the heat is conducted within the material and varies with material and laser wavelength. The better the material conduction (thermal diffusivity) the greater is the extent of the heat affected zone.

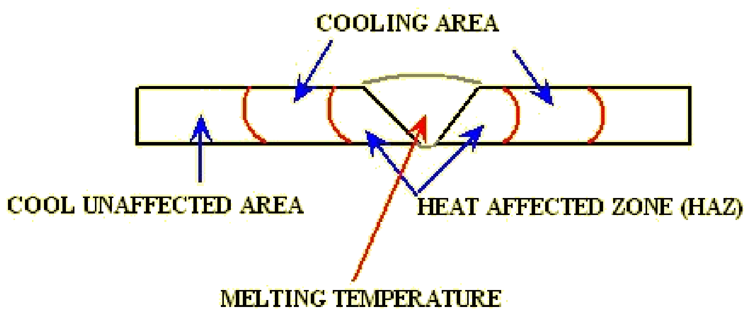

Figure 2.7: Schematic of heat affected zone

Source: Weman (2003)

Not all metals are weldable. For steels, those that alloy steels that can be hardened by heat treatment are generally the hardest to weld, whereas less hardenable plain carbon steels are easier to weld. Welding can also degrade the properties of steels, since welding changes the materials structure and properties in a region of the parent material around the weld called the “heat-affected zone” or HAZ. This can make the welded material in some cases weaker and in other cases making it more brittle. For aluminum welding, lower alloy materials are more easily welded. (Stoebe, 2008).

2.5 THERMOCOUPLE

Temperature is a measure of the average kinetic energy of the particles in a sample of matter, expressed in units of degrees on a homogeneous scale. A number of transducers serve temperature measuring needs and each has advantages and considerations. Thermocouples are the most commonly used sensor type and among the easiest temperature sensors to use and obtain. Thermocouples are a widely used type of temperature sensor in science and industry for measurement and control and can also be used to convert a temperature gradient into electricity. They are based on the Seebeck effect that occurs in electrical conductors that experience a temperature gradient along their length. Thermocouples are used in the manufacture of steel to measure the temperature of the steel in order to determine the carbon content of the steel based on its melting temperature. Thermocouples are typically selected because of their low cost, wide temperature ranges, high temperature limits, and durable nature.

A thermocouple is a device made by two different wires joined at one end, called junction end or measuring end. The two wires are called thermo-elements or legs of the thermocouple. The two thermo-elements are distinguished as positive and negative ones. The other end of the thermocouple is called tail end or reference end is shown in Figure 2.8. (Scervini, 2009).

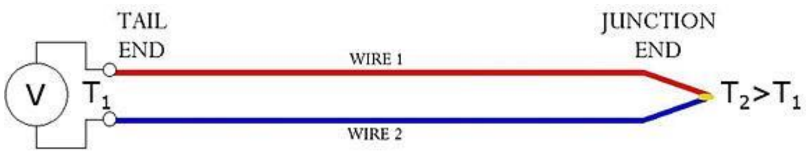

Figure 2.8: Schematic drawing of a thermocouple

Source: Scervini (2009)

There are certain combinations of alloys have become popular as industry standards. Selection of that combination is driven by availability, convenience, stability, melting point, chemical properties, cost, and output. There are many types of thermocouples, each have its own unique characteristics in terms of durability, temperature range, chemical resistance, vibration resistance, and application compatibility. They are usually selected based on the temperature range and sensitivity needed. The most popular type of thermocouple is the type-K. This type is made of Nickel-Chromium versus Nickel-Aluminum wires and has a very wide range of temperature gradients (from -200 °C up to 1300 °C) where the voltage changes almost linear. (Lazaridis, 2010).

2.6 MATERIAL PROPERTIES

There are thousands of materials available for use in engineering applications. Most materials fall into one of three classes that are based on the atomic bonding forces of a particular material. These three classifications are polymeric, ceramic and metallic. Furthermore, different materials can be combined to create a composite material. Within each of these classifications, materials are often further organized into groups based on their chemical composition or certain physical or mechanical properties. Composite materials are often grouped by the types of materials combined or the way the materials are arranged together. (NDT, 2012).

Properties of common solid materials can divided into following categories:

(i) Physical properties: Density, melting and boiling temperature. Metals in general have high electrical conductivity, high thermal conductivity, and high density. Typically they are malleable and ductile, deforming under stress without cleaving. In terms of optical properties, metals are shiny and lustrous. Sheets of metal beyond a few micrometers in thickness appear opaque, but gold leaf transmits green light. (Mortimer, 1975). The melting point is the temperature at which a material changes state from solid to liquid. The melting temperature of an alloy is usually less than the melting temperature of the parent metals.

At the melting point the solid and liquid phase exists in equilibrium. Melting points of some metals and alloys are indicated in the Table 2.1.

(ii) Mechanical Properties: Elastic modulus, shear modulus, Poisson's ratio, yielding stress, ultimate stress, and elongation.

(iii) Thermal Properties: Coefficient of thermal expansion, thermal conductivity. Thermal conductivity is amount of heat passing in unit time through unit surface in a direction normal to this surface when this transfer is driven by unite temperature gradient under steady state conditions. Thermal expansion (coefficient of thermal expansion) is relative increase in length per unite temperature rise. Thermal expansion of metals is generally higher, than that of ceramics. (Kopeliovich, 2012).

(iv) Electric Properties: Electric resistivity.

(v) Acoustic Properties: Compression wave velocity, shear wave velocity, bar velocity.

Table 2.1: Material properties at room temperature

Material	**Melting Point (K)**	**Density (kg/m^3)**	**Specific Heat (J/kg·K)**	**Thermal Conductivity (W/m·K)**	**Thermal Diffusivity ($\times 10^6$ m^2/s)**	**Thermal Expansion Coefficient ($\times 10^{-6}$/°C)**
Aluminum: Pure	933	2702	903	237	97.1	22.5
Alloy 2024-T6 (4.5% Cu, 1.5% Mg, 0.6% Mn)	775	2770	875	177	73.0	23.2
Alloy 195, Cast (4.5% Cu)		2790	883	168	68.2	
Carbon steels: Plain carbon (Mn ≤ 1%, Si ≤ 0.1%)	>3823	7854	434	60.5	17.7	4.14
Mild Carbon	1516	7850	502	65.8		12.06
Stainless steels: AISI 302		8055	480	15.1	3.91	
AISI 304	1670	7900	477	14.9	3.95	17.3
AISI 316		8238	468	13.4	3.48	16.0
AISI 347		7978	480	14.2	3.71	

Source: Incropera et al. (1990)

CHAPTER 3

METHODOLOGY

3.1 INTRODUCTION

This chapter discusses the methodology in this research. It is a body of practices, procedures and rules used by those who work in a discipline or engage in an inquiry and a set of working methods. This chapter is divided into two parts which will describe the analysis of the heat distribution for TWB parts. This chapter focuses on the method to do the project. The method that used in this project is experimental and simulation. The experimental method is use laser welding with contributes test rig and the simulation method that using ABAQUS software.

3.2 PROJECT FLOW CHART

Figure 3.1 shows the flow chart for this research project. It show start to the end of this research project sequences. This research is start with understand the objective of the project. Some literature is studied and the scope of the project is determined. This research used two type of method to analysis the heat transfer which is the experimental and numerical analysis. For experimental method, test rig is designed and fabricated first and then the experimental was carried out. For numerical method, simulation modeling is designed using FE analysis. All result analysis from experiment and simulation is gathered. In discussion, the result from experiment and simulation is compared. Then, the completed report has been submitted to the supervisor examiner for checking and approval.

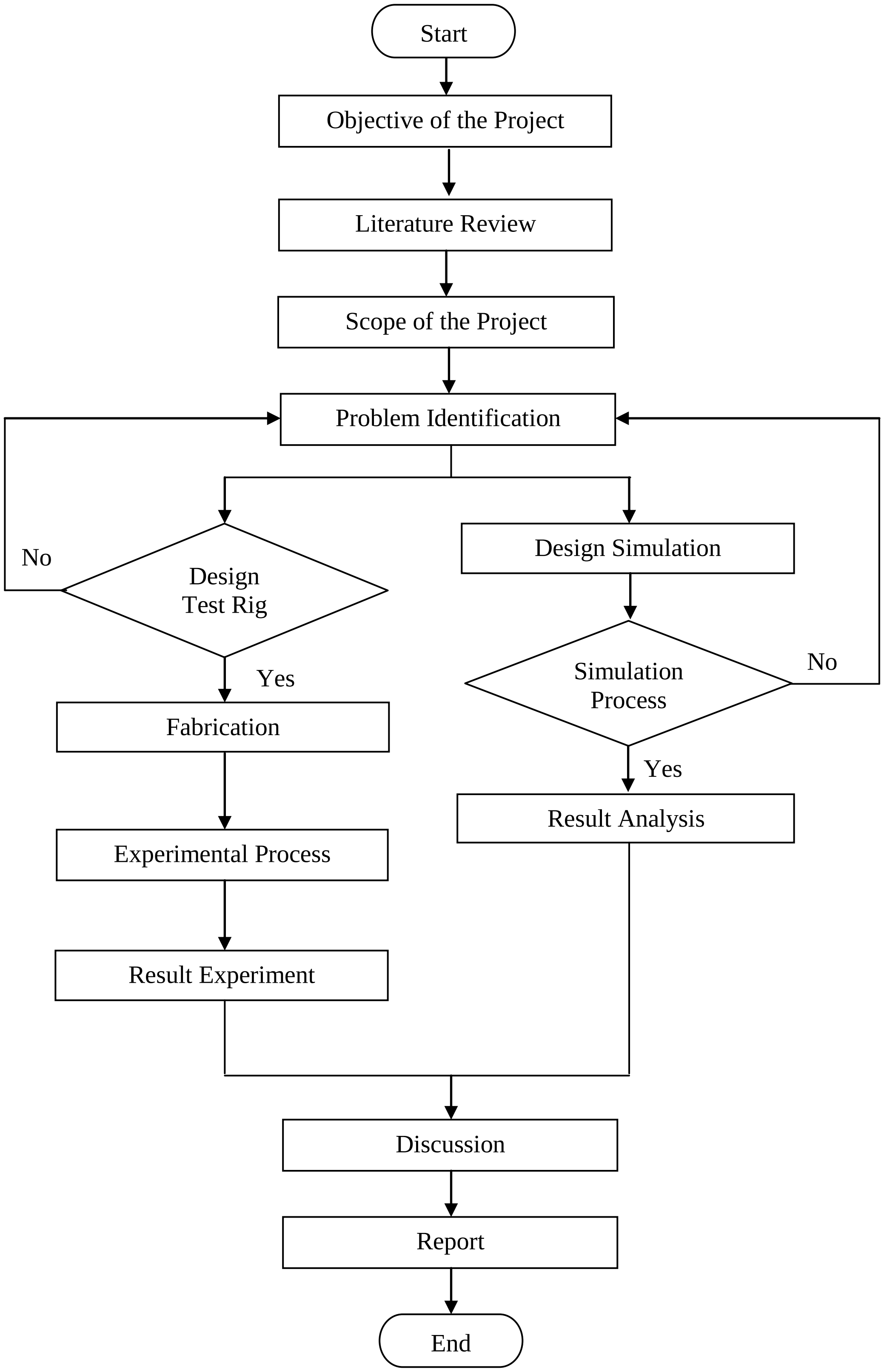

Figure 3.1: Continue project flow chart

3.3 TEST RIG

Test rig is the equipment that used to clamp the specimen material. It produced by some process such as milling, slotting, drilling and others. It also can clamp the material with different thickness. It has several parts that must be assembly. The Design of the test rig must be compliance to several aspects. The design consideration must be done wisely so the design can be fabricated well. The aspects that must be considered in designing the test rig are:

(i) Material Size: Based on the size of the material that available.

(ii) Specimen Size: Test rig is used for testing the specimen (TWB parts) and it must be based on specimen size.

(iii) Machining: To ensure the test rig can be fabricated easily and well.

The ideas for the test rig fabrication are sketched on the paper first to ensure that idea improvement can be made. The final idea is drawn into the Solidworks drawing format with details features (refer to Appendix A). From the sketching drawing, test rig design is transfer to solid modeling and drawing using Solidworks application as better technical drawing as show in Figure 3.2.

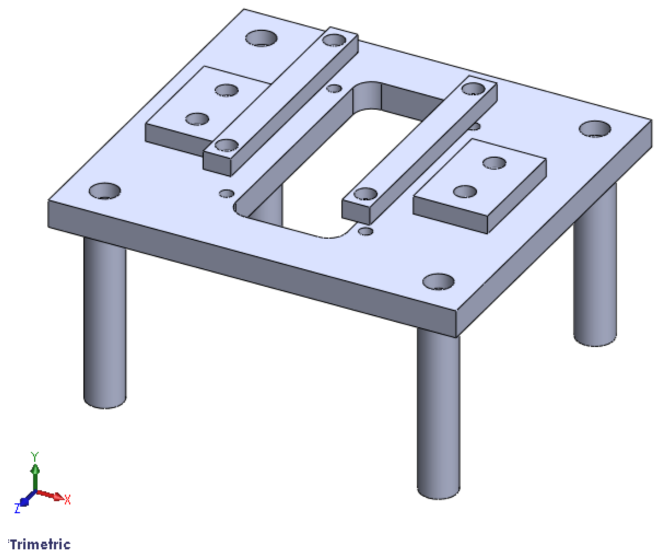

Figure 3.2: Drawing of test rig

The test rig design has four parts such as base, clamper, stopper and base leg as shows in Figure 3.3. Table 3.1 shows the bill of material for test rig. It shows the material used and dimension for each part of test rig. This test rig design using the screw steel for clamping.

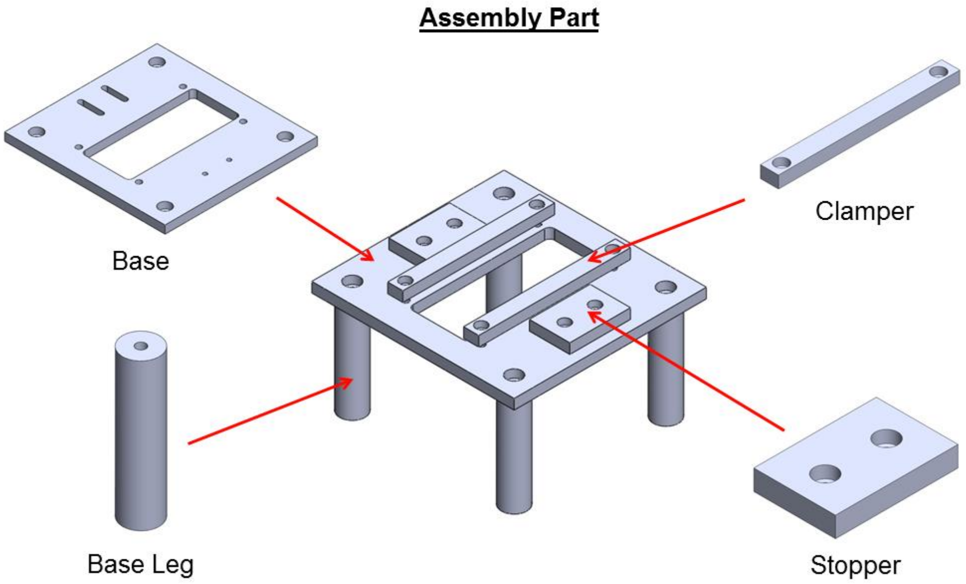

Figure 3.3: Assembly part of test rig

Table 3.1: Bill of material test rig

No.	Part Name	Material	Dimension Size	Quantity
1.	Base	Mild Steel	200 × 190 × 10 mm	1
2.	Clamper	Aluminum	150 × 15 × 10 mm	2
3.	Stopper	Aluminum	60 × 40 × 10 mm	2
4.	Base leg	Aluminum	100 × Dia. 25 mm	4

3.3.1 Fabrication Process

After designing phase, comes fabrication process. This process is about using the material selection and makes the product base on the design and by followed the design dimension. Many methods can be used to fabricate a product, like welding, fastening, cutting, drilling and many more method. Fabrication process is difference from manufacturing process in term of production quantity.

Fabrication process is a process to make only one product rather than manufacturing process that focus to large scale production. Fabrication process was used at the whole system production. This was include part by part fabrication until assembly to others component. Fabrication process needs to be done first in order to make the design come to reality. The fabrication process starts from dimensioning the raw material until it is finish as a desired product.

There is several type of raw material that used to fabricate test rig such as mild steel, aluminum, and aluminum rod used. The raw materials are measured first to desire dimensions based on design specification. Then, it’s cut by use the bandsaw machine. Conventional milling machine as shown in Figure 3.4(a) is used in squaring process as shown in Figure 3.5(a) which is the material is cut and minimized by follow the design dimension. The hole and slot on the base part of test rig is made by using CNC milling machine as shown in Figure 3.4(b). After drilling and slotting process, deburring process is carried out to remove the burr on the test rig part by using a file tool. Removing the burr from the edges of a test rig part will eliminate painful cuts to people handling the material. Tapping process as shown in Figure 3.5(b) is carried out to make thread on the hole for screw by using tapper tool. The size of thread that used on the base test rig is M6. Then, the base leg material is cut and minimized the size based on the desired dimension by using conventional lathe machine in turning process as shown in Figure 3.5(c). Finally, finishing process of the test rig fabrication is made using horizontal grinding machine as shown in Figure 3.5(d). This process is removed the burr and to make smooth surface of the test rig.

(a) (b)

Figure 3.4: (a) Conventional milling machine, (b) CNC milling machine

(a) Squaring process for base plate

(b) Tapping process

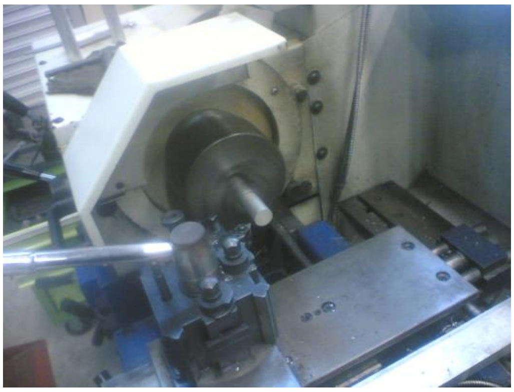

(c) Turning process

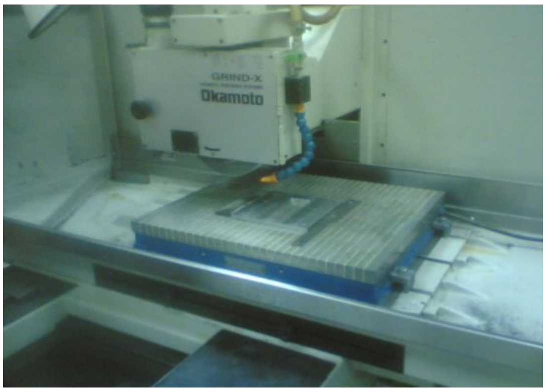

(d) Finishing process

Figure 3.5: Fabrication process

3.3.2 Experimental Setup

Figure 3.6 shows the schematic of the experiment setup. It consists of laser machine as heat source; material specimens to be tested; DASYLab, data logger and thermocouple as measuring tools and test rig as the equipment that used to hold the specimens material. Specimen test used in this study was aluminum 1100 (pure aluminum) with different thickness. The specimens used for the experiment were cut into dimensions 50 width × 100 mm length with various thicknesses of 1, 2 and 3 mm as shows in Figure 3.7. Shearing machine was used to cut the specimens according to dimension. To measure the heat distribution from laser that imposed on the specimen, thermocouple were connected with the measuring device and attached on the specimen.

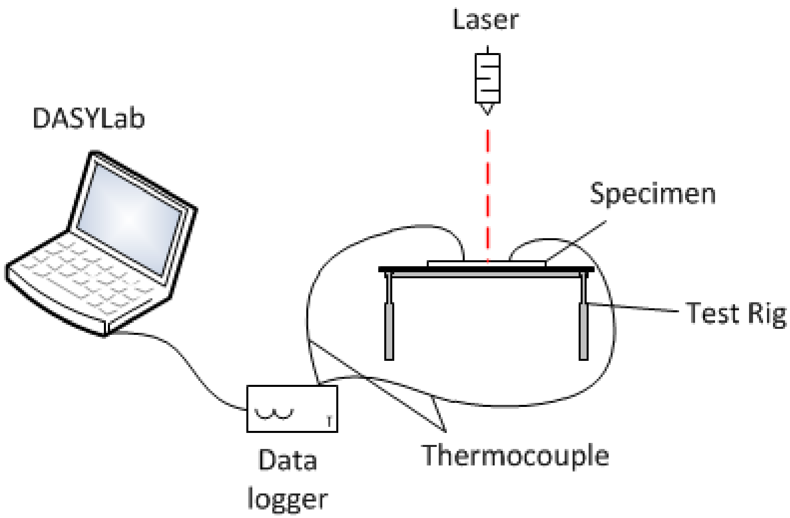

Figure 3.6: Schematic of experimental layout

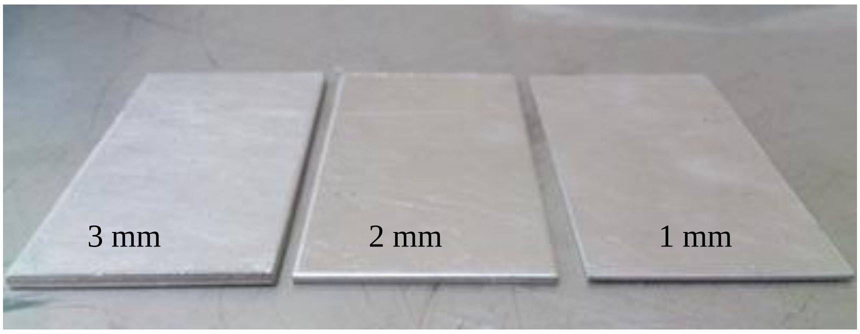

Figure 3.7: Specimen test (Aluminum 1100 material)

Figure 3.8 shows the process to make the hole on the specimen which places thermocouple. This process was done by using EDM super drilling machine and diameter of hole that made is 0.5 mm. The thickness combinations of specimens for each case are shown in Table 3.2.

Table 3.2: Thickness combinations of specimens for each case

Number of Case	Thickness combination
1	3 mm – 1 mm
2	3 mm – 2 mm
3	2 mm – 1 mm

Figure 3.8: Drilling process using EDM super drilling machine

Figure 3.9 shows the position of hole on the specimen. For each thickness, it has 3 holes of point which places thermocouple. Distance from point 1 to the heat source is 1 mm. Then, distance of point 2 to point 1 is 3 mm and followed by the distance point 3 to point 2 is 3 mm too. At this point the temperature will be measured to investigate heat distribution on the specimen.

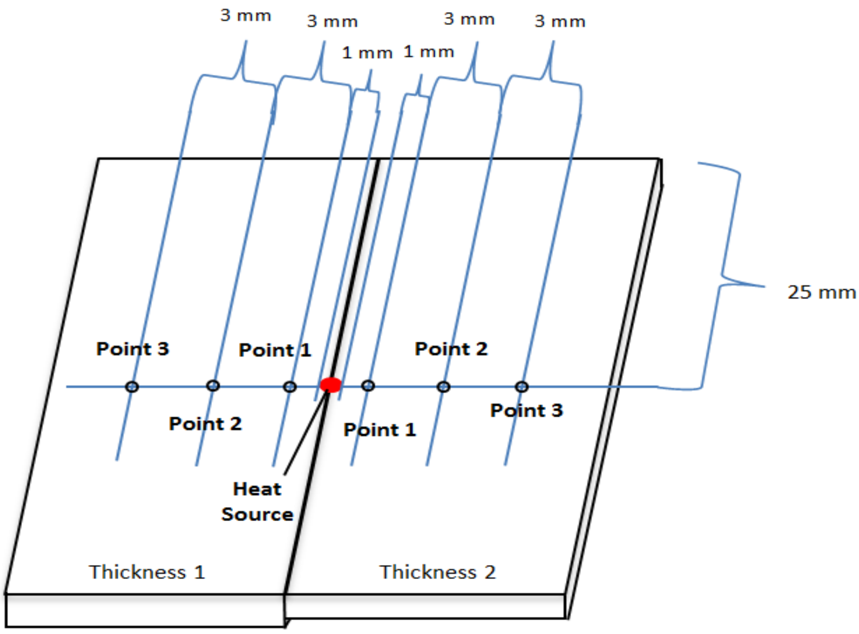

Figure 3.9: Position of points on the specimen

Figure 3.10 shows thermocouple and some tool such as National Instrument (NI 9213) with data logger and DASYLab software is used to conduct the experimental analysis as measuring tools. Technically, a data logger is a device that can be used to store data which use a computer as a real time data recording system. The data from the NI 9123 is stored by data logger and transferred into DASYLab software. The thermocouple type used is type-K due to its ability to withstand at high temperature range -270 to 1350 °C. Using the NI 9213, a compact modular data acquisition system can be created to collect data from up to 16 independent thermocouples. The NI 9213 takes up less space than standard instrumentation in a measurement system and provides more channels for measurement with a sampling rate of 75 samples/second per channel, making the device both compact and efficient for high-channel systems. DASYLab is a popular Easy-To-Use Software in Data Acquisition System with all kinds of interface connected to the hardware. Use DASYLab to interactively create an acquisition, control, simulation or analysis task. It easy to use by simply select a function module and place it on the worksheet. DASYLab supports many data acquisition and control devices, as well as different interfaces that communicate with external instruments.

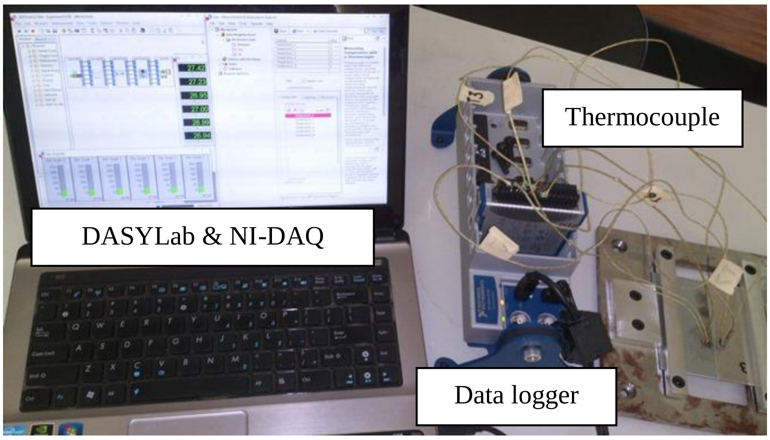

Figure 3.10: Measuring tools component

A laser machine was used as a heat source in investigate heat transfer analysis. The laser welding parameters are shown in Table 3.3. For this study, the condition laser used is unmoved heat source.

Table 3.3: Laser welding parameters

Parameters	Value
Maximum power	75 W
Focus length	96 mm
Heating width	1 mm

3.3.3 Experimental Procedure

Figure 3.11 shows the structure of experimental test that used in this study. There are some equipment used in the experiment such as laser machine, temperature measuring tools and test rig.

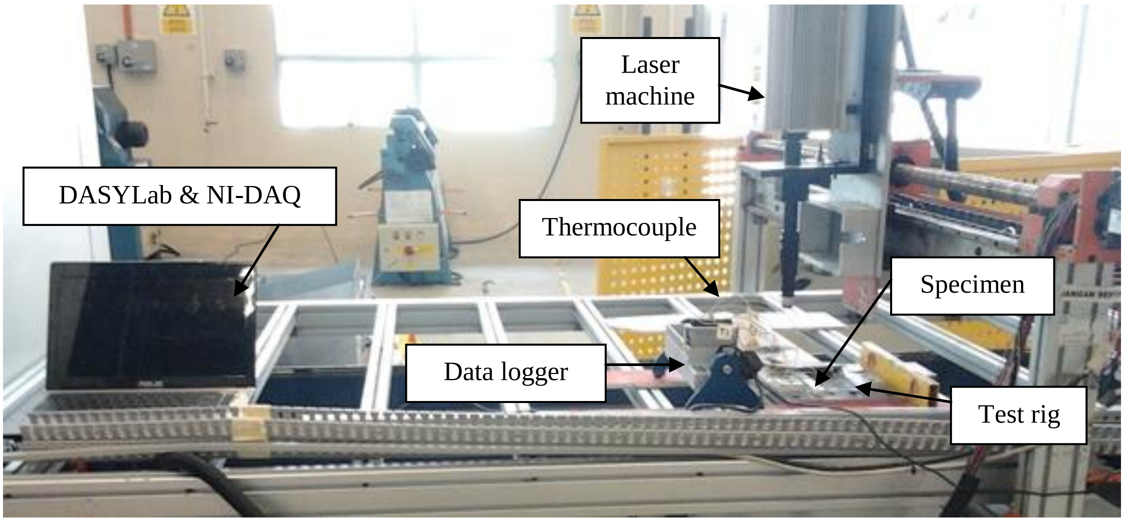

Figure 3.11: Experimental apparatus

The following is the procedure in carrying out the experiment:

(i) Firstly, the specimen was cut into 100 mm length × 50 mm width for every thickness using hydraulic shearing machine.

(ii) Then, 3 holes on each specimen (3 mm distance for each holes point) as place of connecting thermocouple are made by drilling process using EDM super drill machine.

(iii) After that, the specimen is clamped on the test rig, and it’s put under the laser beam. Make sure the laser beam in the middle of the specimen.

(iv) Thermocouple is attached on specimen and to data logger. Then, data logger is connected to computer that has NI-DAQ and DASYLab software.

(v) The laser machine is switched ON and the data from DASYLab software is recorded.

(vi) The specimen test is changed for each different thickness and the data for each experiment is recorded.

3.4 SIMULATION SETUP

This method is using FE software to build the model of TWB parts and create simulation process to analysis heat transfer of that model. FE software used for simulation process is ABAQUS software. ABAQUS software is a suite of software applications for finite element analysis and computer-aided engineering. The software consists of wide material modeling capability, and the program's ability to be customized. In this study ABAQUS it used to simulate the heat transfer during welding. Build the model of heat transfer analysis by drawing the specimen on ABAQUS software with dimension. Before run the simulation analysis, some preparation must be done first which is:

(i) Modeling specimen part is drawn into 50 mm width and various combination of thickness (same as experiment).

(ii) Material properties of aluminium as shown in Table 3.4 are defined for each part. Thermal properties of aluminium at chapter 2 are used in this simulation process.

(iii) Position of heat source is determined as shown in Figure 3.12 and load of heat for condition unmoved heat source is set. The load of heat source used is the load that produces simulation results that is similar to the results in experiment. For this study, the load used is 2×10^6 W/m^2.

(iv) Then, modeling specimen is meshed.

(v) After that, the simulation process is run and the data is recorded at the same point in the experiment.

(vi) Above step is repeated with different size of modeling specimen.

Table 3.4: Thermal properties of aluminium material

Material	Melting Point (K)	Density (kg/m^3)	Specific Heat (J/kg·K)	Thermal Conductivity (W/m·K)	Thermal Diffusivity (×10^6 m^2/s)	Thermal Expansion Coefficient (×10^{-6}/°C)
Aluminum	933	2702	903	237	97.1	22.5

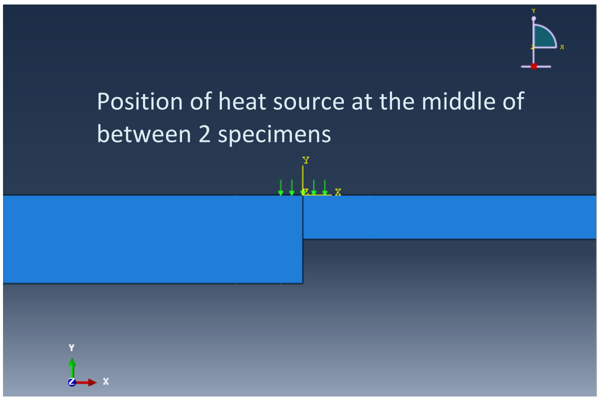

Figure 3.12: Position of heat source on specimen model for simulation

For parametric study, heating position and the value of the heat flux is varied to obtain the optimum welding condition. It means to predict the suitable heating position and heat flux for welding process. Figure 3.13 shows the position of heat that altered. Table 3.5 shows the several parameters that was study.

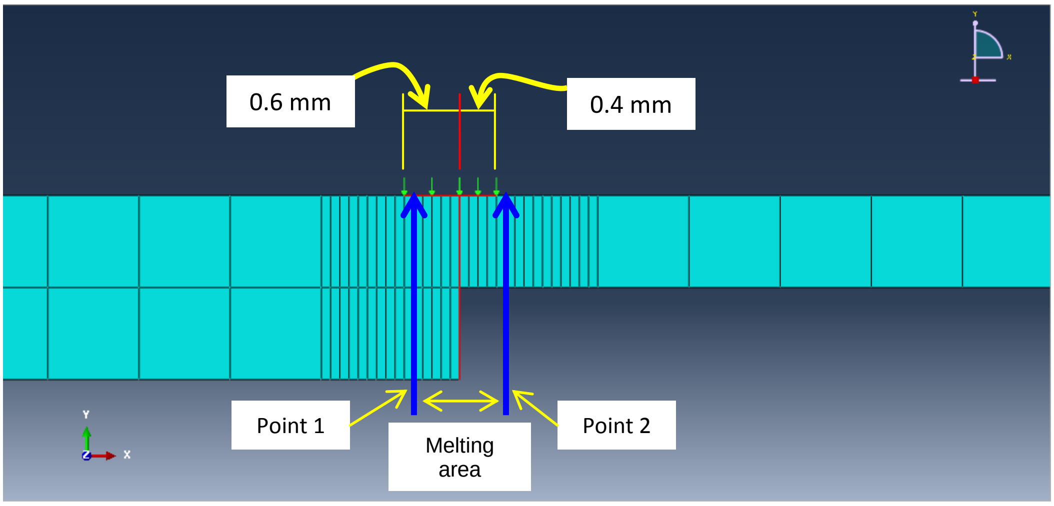

Figure 3.13: Position of heat imposed on modeling specimen for parametric study

Table 3.5: Parametric of heat source

Thickness Combination	**Heating Position**	**Heat Flux (W/m^2)**
3 mm – 1 mm	50% (3 mm) – 50 % (1 mm) 60% (3 mm) – 40 % (1 mm) 70% (3 mm) – 30 % (1 mm)	53×10^6, 54×10^6, 55×10^6
3 mm – 2 mm	50% (3 mm) – 50 % (1 mm) 55% (3 mm) – 45 % (1 mm) 60% (3 mm) – 40 % (1 mm)	61×10^6, 62×10^6, 63×10^6
2 mm – 1 mm	50% (3 mm) – 50 % (1 mm) 55% (3 mm) – 45 % (1 mm) 60% (3 mm) – 40 % (1 mm)	50×10^6, 51×10^6, 52×10^6

CHAPTER 4

RESULTS AND DISCUSSION

4.1 INTRODUCTION

This chapter covers the result and discussion of this research. The final fabrication of the test rig is highlighted in this chapter. Besides that, two type of methods that have been used in this research to investigate heat transfer characteristic for the different thickness of common used type of TWB material which is experimental and simulation. The results of heat transfer from experimental then compared with simulation for validation. The final section of this chapter focuses on the result of parametric study for TWB process.

4.2 TEST RIG FABRICATION

To conduct heat transfer experiment, equipment has been made to hold the specimen material. A complete test rig was built by considering it compatible to place the specimen test. On these requirements, the completed test rig was designed and fabricated as shown in Figure 4.1(a). The overall size of the fabricated test rig is 200 mm length × 190 mm width × 110 mm height. A test rig is the equipment that used to hold the specimens material by clamp it as shows in Figure 4.1(b). This test rig also can use on the specimens that have different thickness.

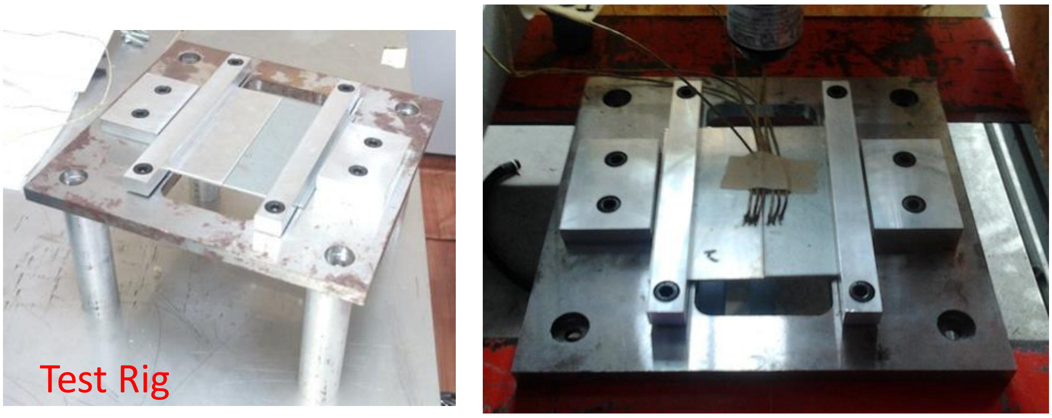

(a) (b)

Figure 4.1: (a) Test rig, (b) Specimens material was clamped on the test rig

There are several important factors were considered during test rig fabrication stages such as material and machining.

(i) Material. Materials used are readily available and must be based on the dimension of design.

(ii) Machining. Using the appropriate machine for each process stage in making a test rig according the design which has been made.

4.3 HEAT TRANSFER ANALYSIS

The results of heat transfer analysis were obtained from this research through experimental test and simulation modeling using finite element method. In experimental, the laser with maximum power 75 W and 1 mm spot size was used for each test. Besides, unmoved heat source was imposed on the aluminum sheet for this study. The specimen materials with combination of various thicknesses used are combination of thickness 3 mm with 1 mm, thickness 3 mm with 2 mm and thickness 2 mm with 1 mm. In this study, a commercial FEA package, ABAQUS, is used to simulate two-dimensional temperature profile of 50 mm width of aluminum material with combination of thickness same as experiment (refer to Appendix B). For the heat source, surface heat flux used is 2×10^6 W/m^2 with unmoved condition. This load was predicted to get the same result with the experiment.

4.3.1 Comparison of Experimental and Simulation

The results of heat transfer from experimental test were compared to verify the results of heat transfer from simulation modeling. From the Figure 4.2, it shows the comparison result between experimental and simulation for thickness of 3 mm with 1 mm. It also shows the temperature distribution of both thicknesses at point 1, 2 and 3. The solid line is represents the temperature line from experimental while dash line represents the temperature line from simulation. Temperatures result from experimental was almost same with simulation result as shows in Table 4.1.

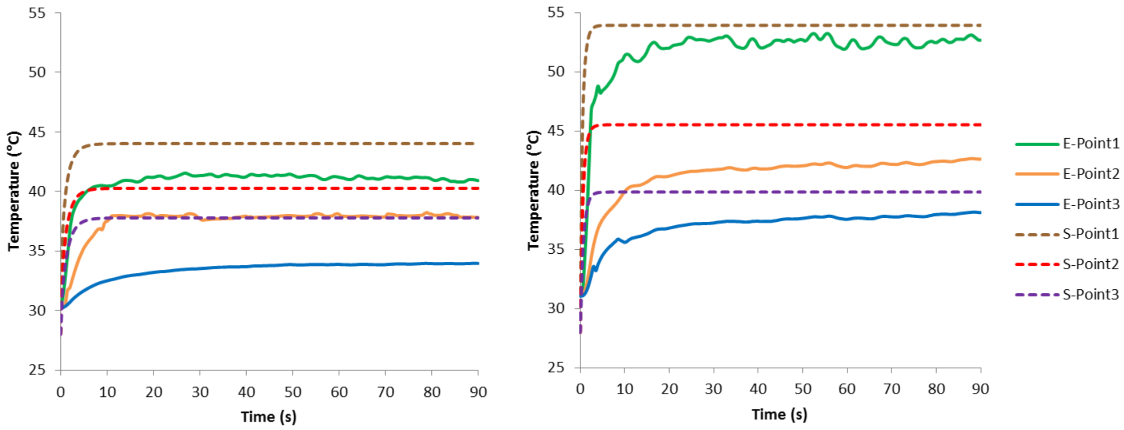

(a) 3 mm thickness (b) 1 mm thickness

Figure 4.2: Comparison result for thickness 3 mm with 1 mm

Table 4.1: Maximum temperature from experimental and simulation for thickness 3 mm with 1 mm

Thickness	Method	Max. Temperature (°C)		
		Point 1	Point 2	Point 3
3 mm	Experiment	41.53	38.22	33.95
	Simulation	44.005	40.2542	37.7721
1 mm	Experiment	53.24	42.67	38.14
	Simulation	53.9275	45.5244	39.8428

From the result obtained, it shows the heat characteristic on different thickness with thin material (1 mm) have a highest temperature than other materials thickness. This is because the thin material is easier to transfer the heat. Percentage of error from different temperature that obtained in experiment and simulation for 3 mm of thickness at point 1 is 5.62 %, at point 2 is 5.05 % and at point 3 is 10.12 %. Whilst, percentage of error from different temperature that obtained in experiment and simulation for 1 mm of thickness at point 1 is 1.27 %, at point 2 is 6.27 % and at point 3 is 4.27 %.

From the Figure 4.3, it shows the comparison result between experimental and simulation for thickness 3 mm with 2 mm. It also shows the temperature distribution of both thicknesses at point 1, 2 and 3. The solid line is represents the temperature line from experimental while dash line represents the temperature line from simulation. Temperatures result from experimental was also almost same with simulation result as shows in Table 4.2.

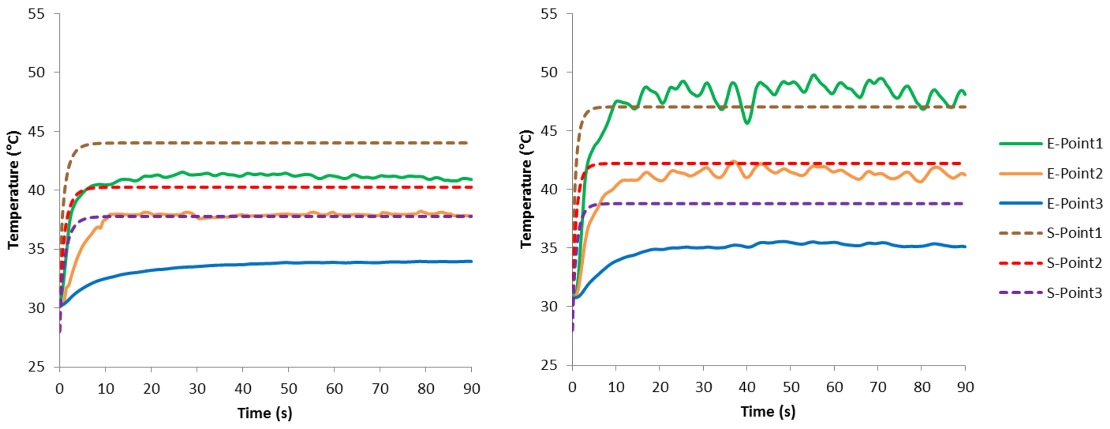

(a) 3 mm thickness (b) 2 mm thickness

Figure 4.3: Comparison result for thickness 3 mm with 2 mm

Table 4.2: Maximum temperature from experimental and simulation for thickness 3 mm with 2 mm

Thickness	Method	Max. Temperature (°C)		
		Point 1	Point 2	Point 3
3 mm	Experiment	41.53	38.22	33.95
	Simulation	44.005	40.2542	37.7721
2 mm	Experiment	49.75	42.39	35.55
	Simulation	47.0299	42.2109	38.7812

From the result obtained, it shows the heat characteristic on different thickness with thin material (2 mm) have a highest temperature than other materials thickness. This is because the thin material is easier to transfer the heat. Percentage of error from different temperature that obtained in experiment and simulation for 3 mm of thickness at point 1 is 5.62 %, at point 2 is 5.05 % and at point 3 is 10.12 %. Whilst, percentage of error from different temperature that obtained in experiment and simulation for 2 mm of thickness at point 1 is 5.78 %, at point 2 is 0.42 % and at point 3 is 8.33 %.

From the Figure 4.4, it shows the comparison result between experimental and simulation for thickness 2 mm with 1 mm. It also shows the temperature distribution of both thicknesses at point 1, 2 and 3. The solid line in the graph is represents the temperature line from experimental while dash line represents the temperature line from simulation. Temperatures result from experimental was almost same with simulation result as shows in Table 4.3.

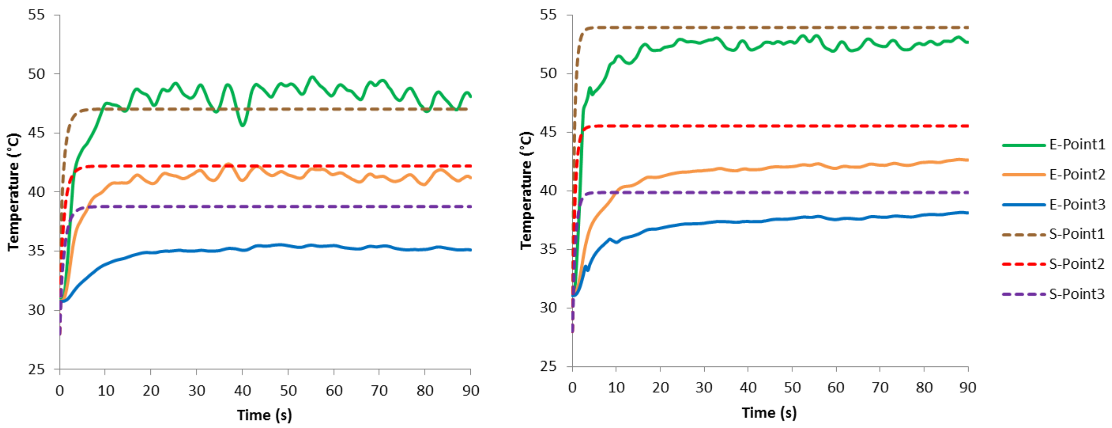

(a) 2 mm thickness (b) 1 mm thickness

Figure 4.4: Comparison result for thickness 2 mm with 1 mm

Table 4.3: Maximum temperature from experimental and simulation for thickness 2 mm with 1 mm

Thickness	**Method**	**Max. Temperature (°C)**		
		Point 1	**Point 2**	**Point 3**
2 mm	Experiment	49.75	42.39	35.55
	Simulation	47.0299	42.2109	38.7812
1 mm	Experiment	53.24	42.67	38.14
	Simulation	53.9275	45.5244	39.8428

From the result obtained, it shows the heat characteristic on different thickness with thin material (1 mm) have a highest temperature than other materials thickness. This is because the thin material is easier to transfer the heat. Percentage of error from different temperature that obtained in experiment and simulation for 2 mm of thickness at point 1 is 5.78 %, at point 2 is 0.42 % and at point 3 is 8.33 %. Whilst, percentage of error from different temperature that obtained in experiment and simulation for 1 mm of thickness at point 1 is 1.27 %, at point 2 is 6.27 % and at point 3 is 4.27 %.

From the graph comparison of the result experimental and simulation, it shows the different of temperature for each thickness of material have small percentage of different. This is because there are several factors that cause these differences such as use of unstable laser power in the experiment, efficiency of laser machine and the occurrence of heat loss during carry out the experiment.

4.4 PARAMETRIC STUDY

Several parameters have been studied in this research. The parameters studied were such as position of the heat source and amount of surface heat flux consumption in TWB process. These investigations have led to an optimum welding condition proposed for weld the aluminum material. The condition proposed is to get the balanced melting area on both thicknesses combination for 1 mm spot size. The melting temperature for aluminum material is 660 °C.

Figure 4.5 shows the temperature's distribution at different heating positions and amount of heat flux for thickness 3 mm with 1 mm. Point 1 which represents the blue color is the temperature point at the thickness material of 3 mm was measured. While point 2 represents the red color is the temperature point at the thickness material of 1 mm was measured. Dashed green line in the graph shows the temperature of melting point. There are three different heating positions that were investigated for this combination thickness which is 50 % on 3 mm thickness region and 50 % on 1 mm thickness region (Figure 4.5(a)), 60 % on 3 mm thickness region and 40 % on 1 mm thickness region (Figure 4.5(b)), and 70 % on 3 mm thickness region and 30 % on 1 mm thickness region (Figure 4.5(c)).

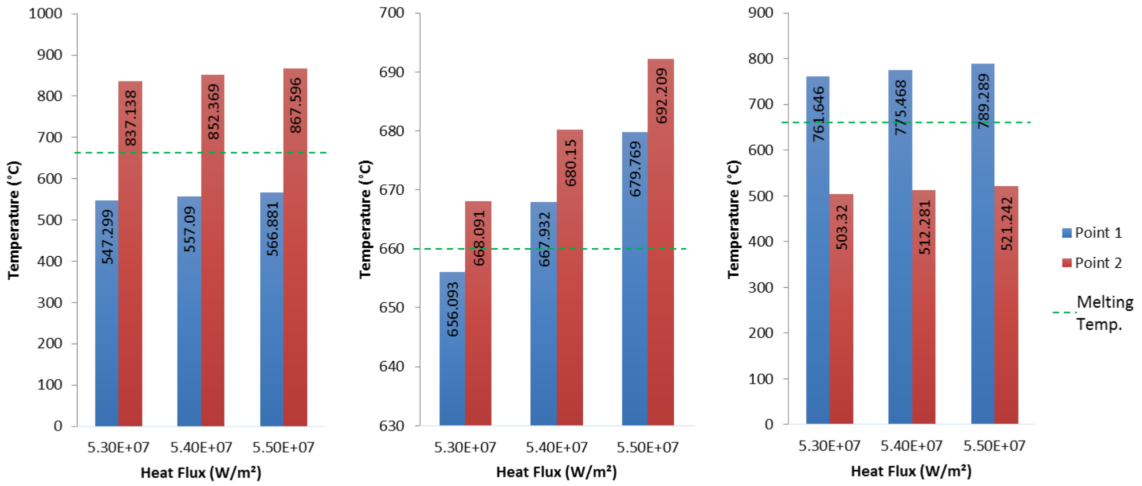

(a) Position 50% - 50% (b) Position 60% - 40% (c) Position 70% - 30%

Figure 4.5: Temperature distribution for different position of heating and heat flux on thickness 3 mm with 1 mm

It is observed that the heating position at 60 % on 3 mm thickness region and 40 % on 1 mm thickness region (Figure 4.5(b)) had the temperature that reached the melting point for each point of thickness with heat flux used are 54 × 10^6 W/m^2 and 55 × 10^6 W/m^2. For optimum welding condition the temperature at point 1 and point 2 must had reached the melting point but not too high to avoid unbalance of melting area. So, the better position of heating and amount of heat flux used is at 60 % on 3 mm thickness region and 40 % on 1 mm thickness region with 54 × 10^6 W/m^2 of heat flux as shows at Appendix C1. Temperature at point 1 and point 2 for optimum welding condition are 667.329 °C and 680.15 °C respectively.

Figure 4.6 shows the temperature's distribution at different heating positions and amount of heat flux for thickness 3 mm with 2 mm. Point 1 which represents the blue color is the temperature point at the thickness material of 3 mm was measured. While point 2 represents the red color is the temperature point at the thickness material of 2 mm was measured. Dashed green line in the graph shows the temperature of melting point. There are three different heating positions that were investigated for this combination thickness which is 50 % on 3 mm thickness region and 50 % on 2 mm thickness region (Figure 4.6(a)), 55 % on 3 mm thickness region and 45 % on 2 mm thickness region (Figure 4.6(b)), and 60 % on 3 mm thickness region and 40 % on 2 mm thickness region (Figure 4.6(c)).

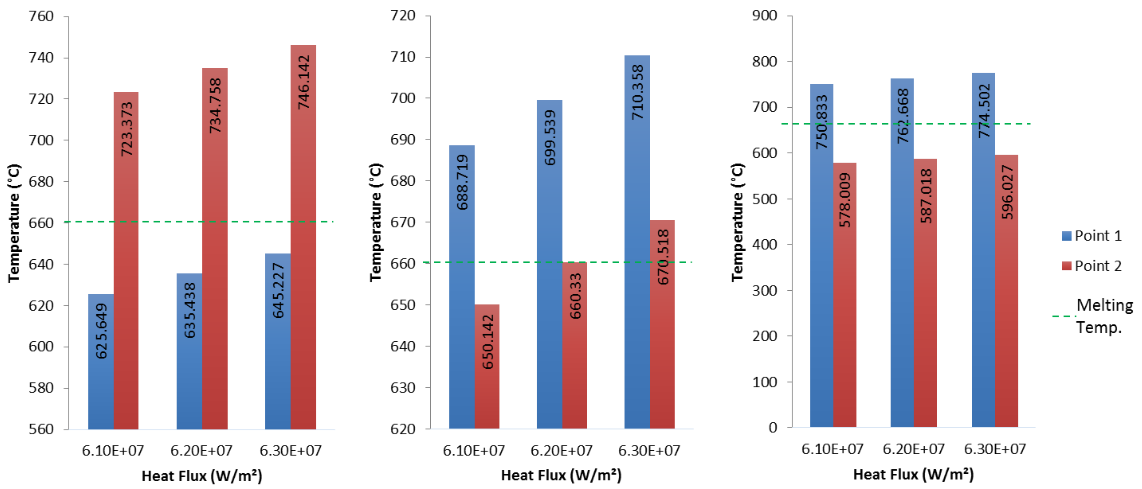

(a) Position 50% - 50% (b) Position 55% - 45% (c) Position 60% - 40%

Figure 4.6: Temperature distribution for different position of heating and heat flux on thickness 3 mm with 2 mm

It is observed that the heating position at 55 % on 3 mm thickness region and 45 % on 2 mm thickness region (Figure 4.6(b)) had the temperature that reached the melting point for each point of thickness with heat flux used are 62×10^6 W/m^2 and 63×10^6 W/m^2. For optimum welding condition the temperature at point 1 and point 2 must had reached the melting point but not too high to avoid unbalance of melting area. So, the better position of heating and amount of heat flux used is at 55 % on 3 mm thickness region and 45 % on 2 mm thickness region with 62×10^6 W/m^2 of heat flux as shows at Appendix C2. Temperature at point 1 and point 2 for optimum welding condition are 699.539 °C and 660.33 °C respectively.

Figure 4.7 shows the temperature's distribution at different heating positions and amount of heat flux for thickness 2 mm with 1 mm. Point 1 which represents the blue color is the temperature point at the thickness material of 2 mm was measured. While point 2 represents the red color is the temperature point at the thickness material of 1 mm was measured. Dashed green line in the graph shows the temperature of melting point. There are three different heating positions that were investigated for this combination thickness which is 50 % on 2 mm thickness region and 50 % on 1 mm thickness region (Figure 4.7(a)), 55 % on 2 mm thickness region and 45 % on 1 mm thickness region (Figure 4.7(b)), and 60 % on 2 mm thickness region and 40 % on 1 mm thickness region (Figure 4.7(c)).

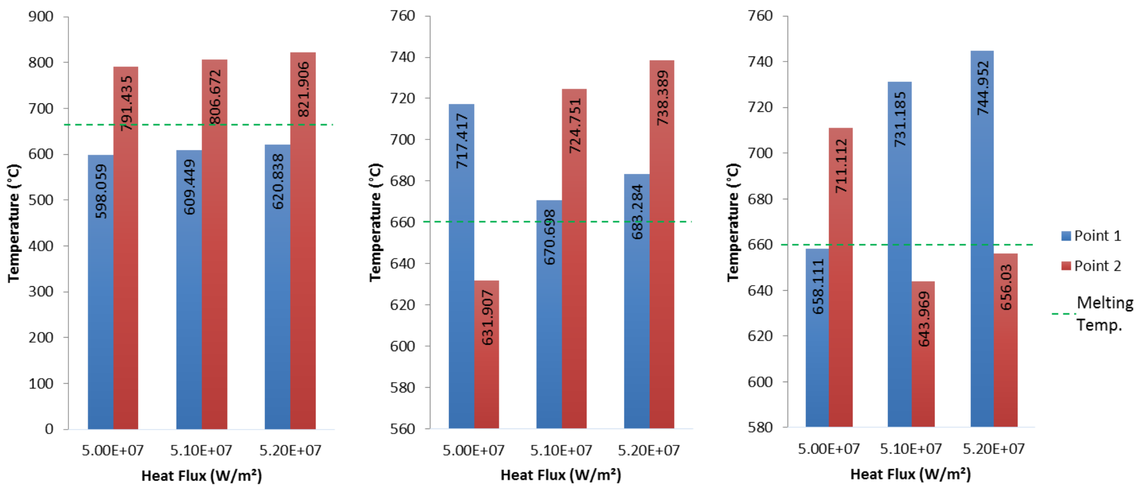

(a) Position 50% - 50%　　(b) Position 55% - 45%　　(c) Position 60% - 40%

Figure 4.7: Temperature distribution for different position of heating and heat flux on thickness 2 mm with 1 mm

It is observed that the heating position at 55 % on 2 mm thickness region and 45 % on 1 mm thickness region (Figure 4.7(b)) had the temperature that reached the melting point for each point of thickness with heat flux used are 51×10^6 W/m^2 and 52×10^6 W/m^2. For optimum welding condition the temperature at point 1 and point 2 must had reached the melting point but not too high to avoid unbalance of melting area. So, the better position of heating and amount of heat flux used is at 55 % on 2 mm thickness region and 45 % on 1 mm thickness region with 51×10^6 W/m^2 of heat flux as shows at Appendix C3. Temperature at point 1 and point 2 for optimum welding condition are 667.329 °C and 680.15 °C respectively.

4.4.1 Optimum Parameter

From the parametric study, the optimum of heating position and amount of heat flux was obtained as shown in Table 4.4. This optimum parameter must consider in TWB process to get the optimum welding condition.

Table 4.4: Optimum parameters

Thickness (mm)	Heating Position	Heat Flux (W/m^2)
3 – 1	3 mm – 60 % 1 mm – 40 %	54×10^6
3 – 2	3 mm – 55 % 2 mm – 45 %	62×10^6
2 – 1	2 mm – 55 % 1 mm – 45 %	51×10^6

Combination thickness of 3 mm with 2 mm and 2 mm with 1 mm has same thickness ratio. This combination also has same optimum heating position but the heat flux is different.

CHAPTER 5

CONCLUSIONS AND RECOMMENDATIONS

5.1 INTRODUCTION

For the final chapter it represent about conclusion and recommendation for the research. In this chapter will cover the conclusion of the research, concluding all the result that obtained. Besides that this chapter also contains recommendation about the research. From this recommendation the improvements can be made in the future for this kind of research.

5.2 CONCLUSIONS

Test rig has been fabricated and used in the heat transfer experiment. In this study, the heat profile of aluminum 1100 under three different type of thickness combination, 3 mm - 1 mm, 3 mm – 2 mm and 2 mm - 1 mm was examined. Heat transfer analysis has been conducted on this combination of different thickness using the laser machine with low capacity of 75 W. FE analyses also has been carried out with the model designed as the same as the specimens in experiment to simulate the heat transfer modeling. The results indicate that, the thin material has higher temperature than thick material because it is easier to transfer the heat. From the acquired results, it can be concluded Finite Element Analysis can be used to do comparison with experimental. It because the result of the graphs compared are nearly the same. Comparing experimental data with simulation data is validated with the small percentage of error which is less than 11 %. Error occurred due to the use of unstable laser power and the occurrence of heat loss during carry out the experiment.

Further, parameters studied in this research are heating position and heat flux. From this research, the joining in different thickness can produce by using laser welding with find the optimum weld position. Different combination of material thickness requires different heating positions including heat flux used. Each combination of thickness has use different heat flux to get the balance melting area for TWB process. Increasing the thickness of the material is increases the use of heat flux. However, it can be concluded from these results that the FE method used can predict the heat distribution of the material with different thickness.

5.3 RECOMMENDATIONS AND FURTHER RESEARCH

The recommendations are based on the problems encountered in this study. There are few recommendations which can be implemented in order to improve this research in the future. To extend our knowledge on TWB process, further research is proposed as below:

(i) Experiment using a high intensity laser. Use of high intensity laser, the welding process in TWB can be performed on real situation. Study the microstructure of the material can be analysing when the welding process can be performed.

(ii) Investigate heat transfer characteristic on material other than aluminum material with different thickness.

(iii) Advanced FE analysis for the dynamic heat source. This analysis can be done in 3D modeling with moveable heat source. With this analysis many parameter can be investigated such as heating speed and heating time.

REFERENCES

Auto/Steel Partnership. 1995. Tailor welded blank design and manufacturing manual. Technical Report.

Bouaifi, B. and Sommer, D. 1997. Influence of joining techniques on the microstructure and formability of steel sheet. *Welding Research Abroad.* **42**(3): 37-40.

Brown, K. R., Venie, M. S. and Woods, R. A. 1995. The increasing use of aluminum in automotive applications. *Journal of Metals*. **47**(7): 20-23.

Clapham, L., Abdullah, K., Jeswiet, J.J., Wild, P.M. and Rogge, R. 2004. Neutron diffraction residual stress mapping in same gauge and differential gauge tailor welded blanks. *Journal of Materials Processing Technology*. **148**(2): 177-185.

Das, S. 2000. Aluminum tailor welded blanks. *Advanced Materials and Processing*. **157**(3): 41-2.

Davies, R.W., Vetrano, J.S., Smith, M.T. and Pitman, S.G. 2002. Mechanical properties of aluminum tailor welded blanks at superplastic temperatures. *Journal of Materials Processing Technology*. **128**(1-3): 38-47.

Garmo, P.P.D. 1974. *Material and process in manufacturing*, (4th ed.). New York: Macmillan Publishing Cooperation Co.

Kopeliovich, D. 2012. Physical properties of metals (online). http://www.substech.com (10 December 2012).

Grande, B., Wærstad, O. and Runeborg, P. 2012. Weld setup, variable frequency and heat affected zones in high frequency tube and pipe welding. Norway: July.

Heo, Y.M., Wang, S.H., Kim, H.Y. and Seo, D.G. 2001. The effect of the drawbead dimensions on the weld-line movements in the deep drawing of tailor welded blanks. *Journal Material Process Technology*. **113**: 686-691.

Huntington, C.A. and Eagar, T.W. 1982. Laser welding of Aluminum and Aluminum Alloys. *Welding Journal*. **62**(4): 105s.

Incropera, F.P and DeWitt, D.P. 1990. *Fundamentals of heat and mass transfer*. (3rd ed.). John Wiley & Sons, Inc.

Karagiannis, S. and Chryssolouris, G. 2003. Nd:YAG laser welding: an overview. Proc. SPIE 5131. *Third GR-I International Conference on New Laser Technologies and Applications*. United States: 16 February.

Kinsey, B., Liu, Z. and Cao, J. 2000. A novel forming technology for tailor welded blanks. *Journal of Materials Processing Technology*. **99**: 145-153.

KM (Key to Metals). 2009. Laser Welding of Aluminum and Aluminum Alloys: Part One (online). http://www.keytometals.com/page.aspx?ID=CheckArticle&site=ktn&NM=214 (8 December 2012).

Lazaridis, G. 2010. How Thermocouple works (online). http://www.pcbheaven.com (5 December 2012).

Li, J. 2010. The effect of weld design on the formability of laser tailor welded blanks. Master Thesis. University of Waterloo, Canada.

Mallieswaran, K., Siranjeevi, L. and Premkumar, R. 2012. Study of weld-line movements for the deep drawing process of tailor welded blanks. *Journal of Advanced Technology in Engineering*. **1**(1): 76-80.

Meinders, V.T., Berg, A.V.D. and Huétink, J. 2000. Deep drawing simulations of tailored blanks and experimental verification. *Journal of Materials Processing Technology*. **103**(1): 65-73.

Migliore, L. 1998. The principles of laser welding. Ind. Laser Rev. **13**(7): 17-21.

Mortimer, C.E. 1975. *Chemistry: A conceptual approach*. (3rd ed.). New York: D. Van Nostrad Company.

NDT Resource Center. 2012. Material and process (online). http://www.ndt-ed.org/EducationResources/CommunityCollege/Materials/cc_mat_index.htm (5 December 2012).

Padmanabhan, R., Oliveira, M.C. and Menezes, L.F. 2006. Deep drawing of aluminum-steel tailor-welded blanks. *Journal of Materials and Design*. **29**(1): 154-160.

Pallet, R.J. and Lark, R.J. 2001. The use of tailored blanks in the manufacture of construction components. *Journal of Materials Processing Technology*. **117** (1-2): 249-254.

Panda, S.K., Kumar, D.R., Kumar, H. and Nath, A.K. 2007. Characterization of tensile properties of tailor welded IF steel sheets and their formability in stretch forming. *Journal of Materials Processing Technology*. **183**(2-3): 321-332.

Qi, Y. 2012. The new technology in the automotive industry by using tailor welded blanks (online). http://www.baosteel.com/english_n/e07technical_n/21be.pdf (28 November 2012).

Rojek, J., Hyrcza-Michalska, M., Bokota, A. and Piekarsk, W. 2012. Determination of mechanical properties of the weld zone in tailor-welded blanks. *Archives of Civil and Mechanical Engineering*. **12**(2): 156-162.

Rooks, B. 2001. Tailor-welded blanks bring multiple benefits to car design. *Assembly Automation*. **21**(4): 323-328.

Saunders, F.I. and Wagoner, R.H. 1995. The use of tailor-welded blanks in automotive applications. The Ohio State University, USA.

Saunders, F.I. and Wagoner, R.H. 1996. Forming of tailor-welded blanks. *Metallurgical and Materials Transactions A: Physical Metallurgy and Materials Science*. **27A**(9): 2605-2616.

Scervini, M. 2009. Thermocouples: The operating principle. *Thermoelectric Materials for Thermocouples*. University of Cambridge, UK.

Schuöcker, D. 1998. Handbook of the EuroLaser Academy Vol.2. London: Chapman & Hall.

Siemens. 2013a. CAE/Computer-Aided Engineering (online). http://www.plm. automation.siemens.com/en_us/plm/cae.shtml (4 January 2013).

Siemens. 2013b. FEA/Finite Element Analysis (online). http://www.plm. automation.siemens.com/en_us/plm/fea.shtml (4 January 2013).

Smith, M. 2012. BoronExtrication.com. B-Pillar 'Tailor Rolled' to 8 Different Thicknesses (online). http://boronextrication.com/2012/11/b-pillar-tailor-rolled-to-8-different-thicknesses/ (10 May 2013).

Stoebe, T.G. 2008. Welding Introduction. Slide. University of Washington, USA.

Thasanaraphan, P. 2012. A study on the welding characteristics of tailor welded blank metal sheets using gtaw and laser welding. *Theses and Dissertations*. **1097**.

TTB (Thyssenkrupp Tailored Blanks). 2012. Product range (online). http://www.thyssenkrupptailoredblanks.it/ (6 December 2012).

Weman, K. 2003. Welding processes handbook. New York: CRC Press LLC.

APPENDICES

APPENDIX A

PARTS DRAWING

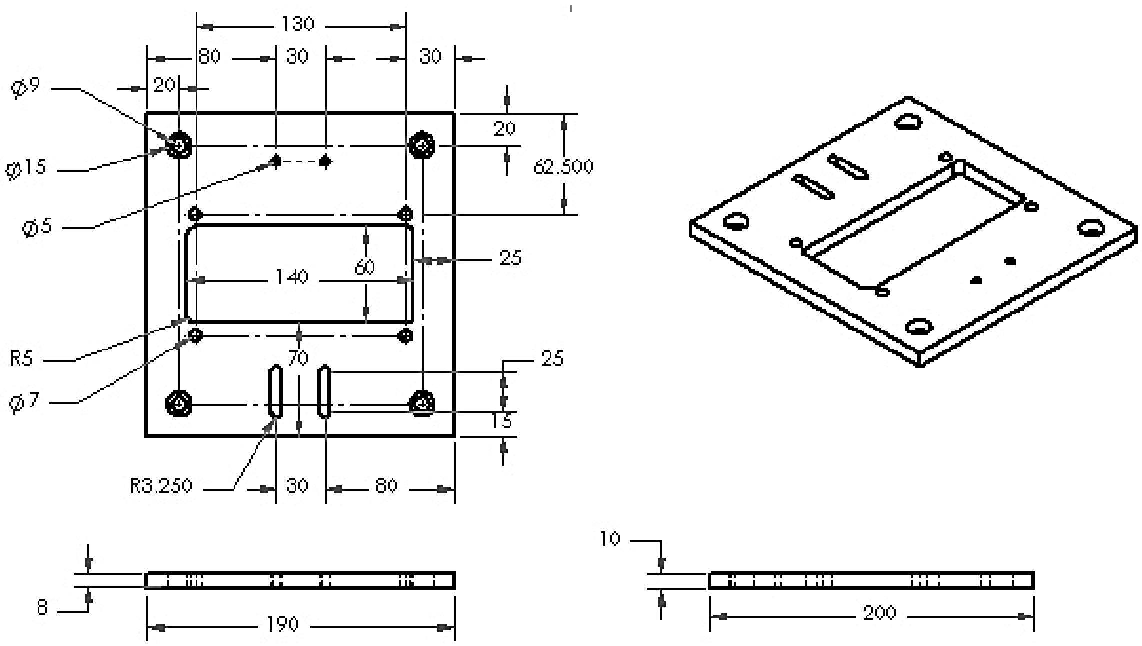

Figure A.1: Base part

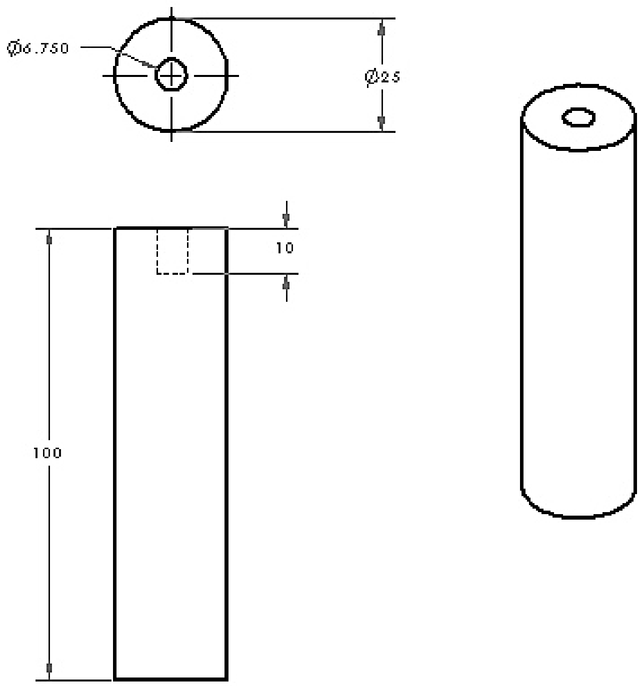

Figure A.2: Base leg part

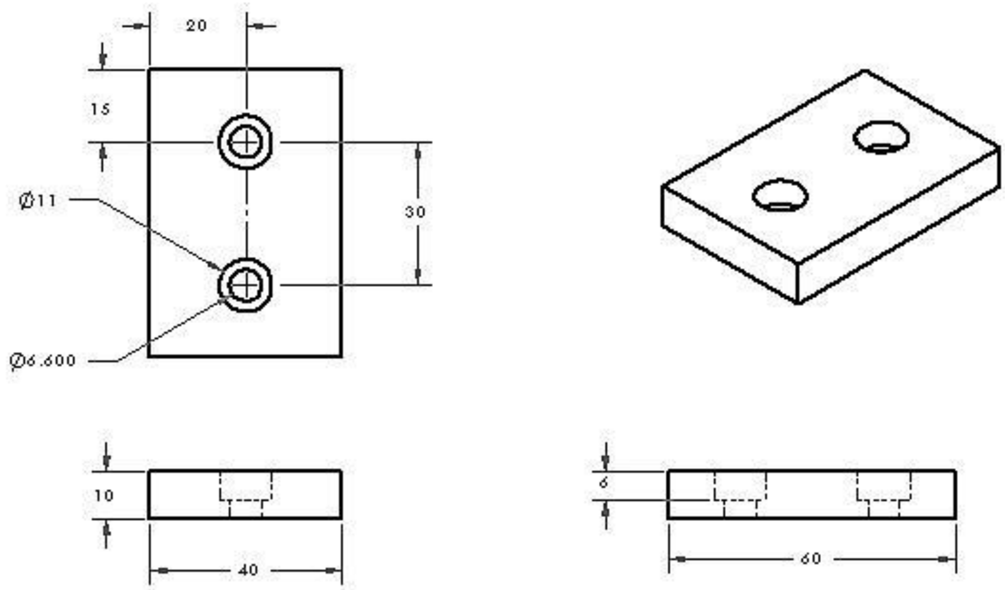

Figure A.3: Stopper part

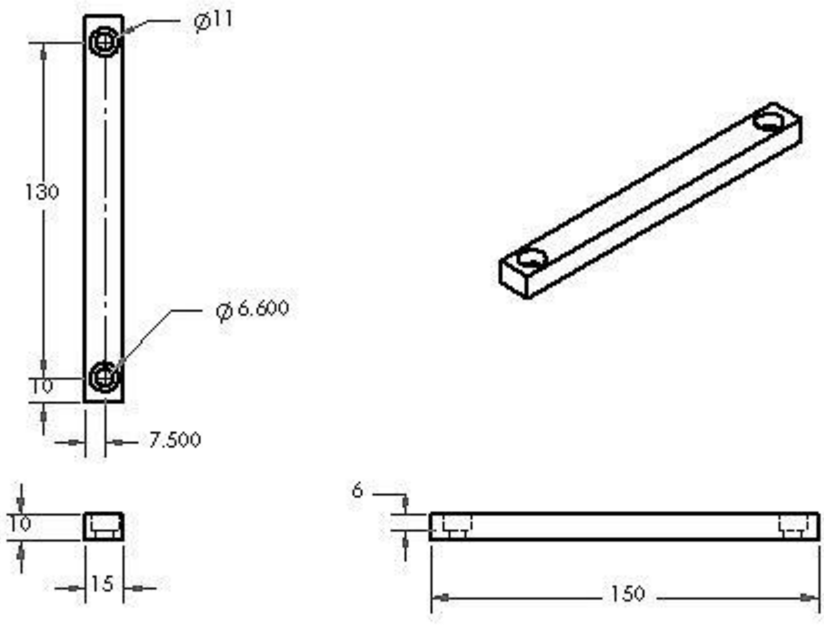

Figure A.4: Clamper part

APPENDIX B

SIMULATION FIGURES

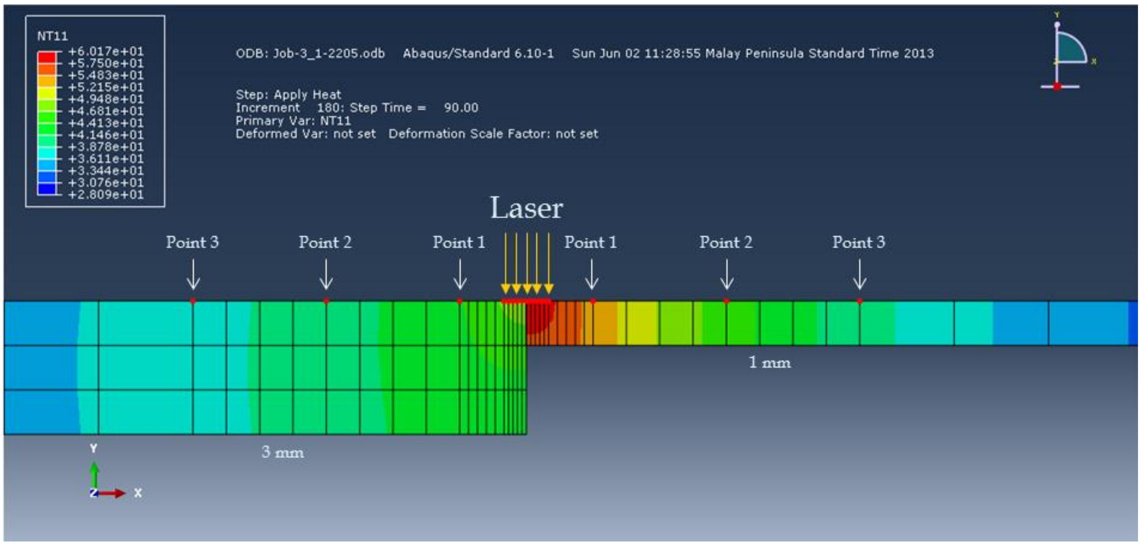

Figure B.1: Thickness 3 mm with 1 mm.

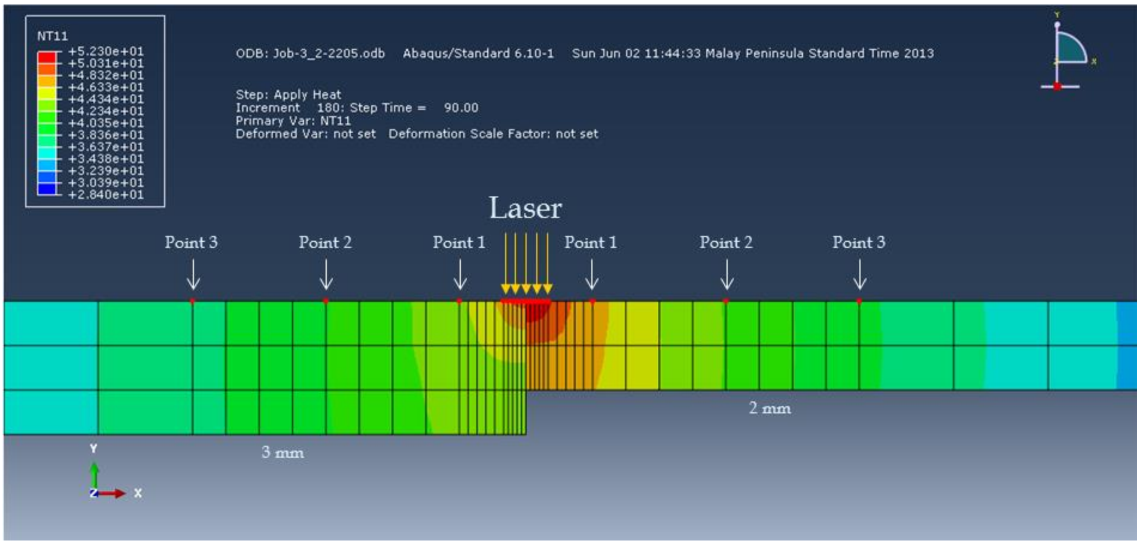

Figure B.2: Thickness 3 mm with 2 mm.

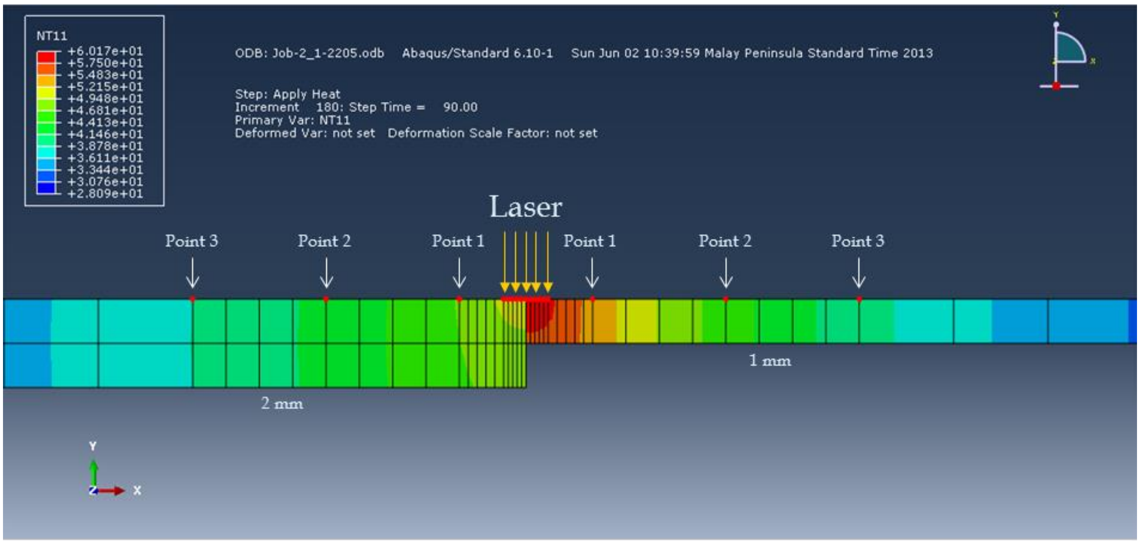

Figure B.3: Thickness 2 mm with 1 mm.

APPENDIX C1

PARAMETRIC STUDY ON THICKNESS OF 3 mm AND 1 mm

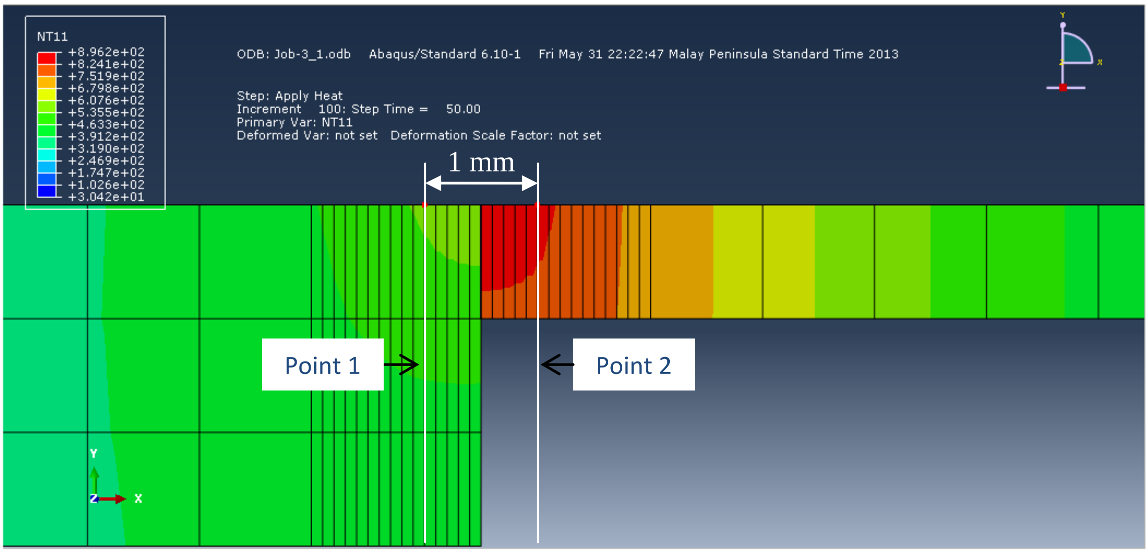

(a) Heating position at 50 % (3 mm) and 50 % (1 mm) with 54 × 10^6 W/m^2 of heat flux

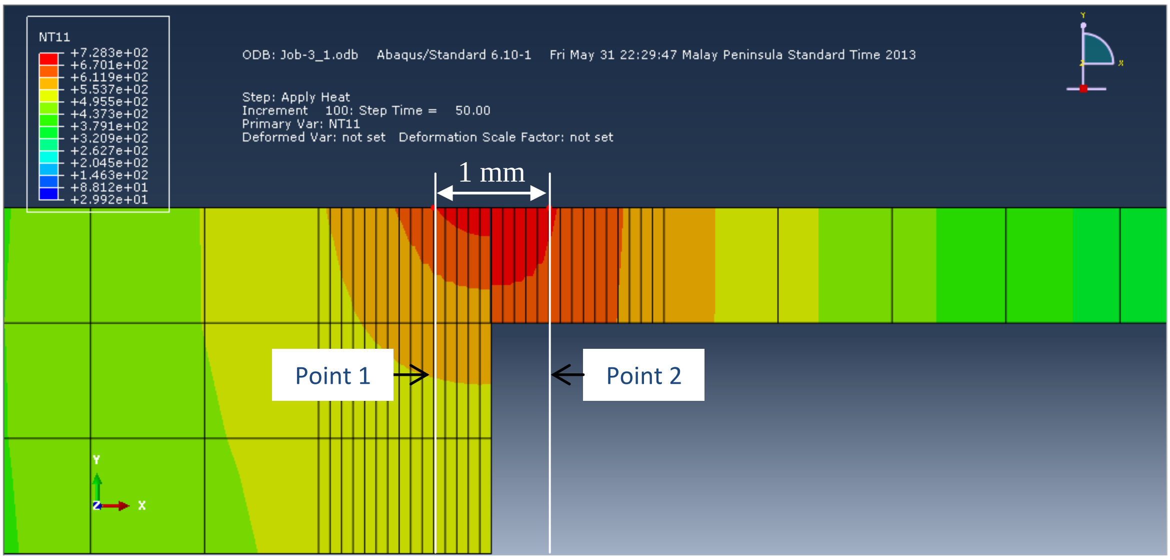

(b) Heating position at 60 % (3 mm) and 40 % (1 mm) with 54 × 10^6 W/m^2 of heat flux

Figure C.1: Different heating position with 54 × 10^6 W/m^2 of heat flux

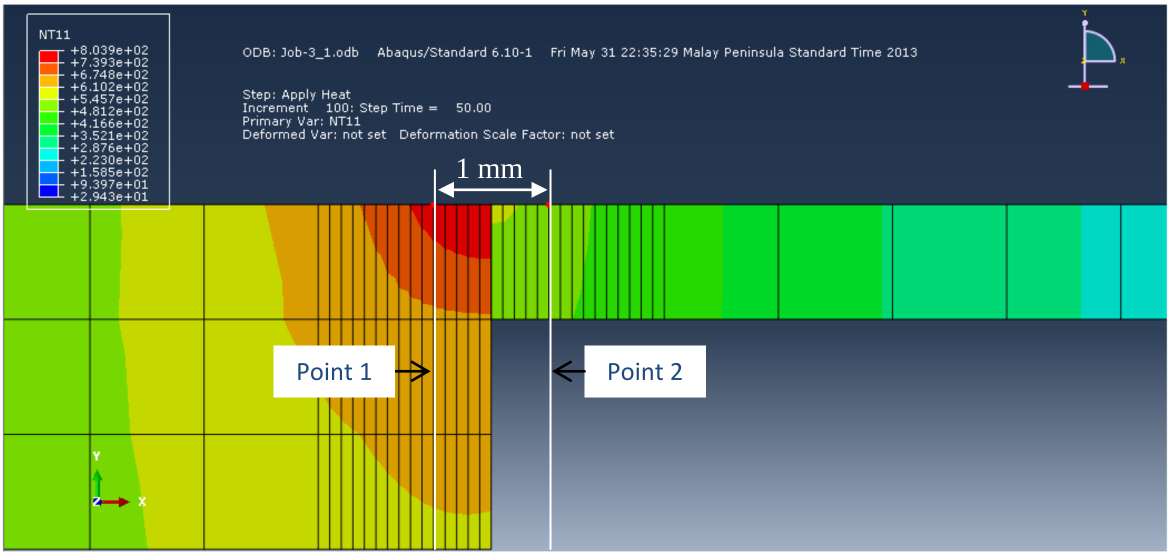

(c) Heating position at 70 % (3 mm) and 30 % (1 mm) with 54 × 10^6 W/m^2 of heat flux

Figure C.1: Continued

APPENDIX C2

PARAMETRIC STUDY ON THICKNESS OF 3 mm AND 2 mm

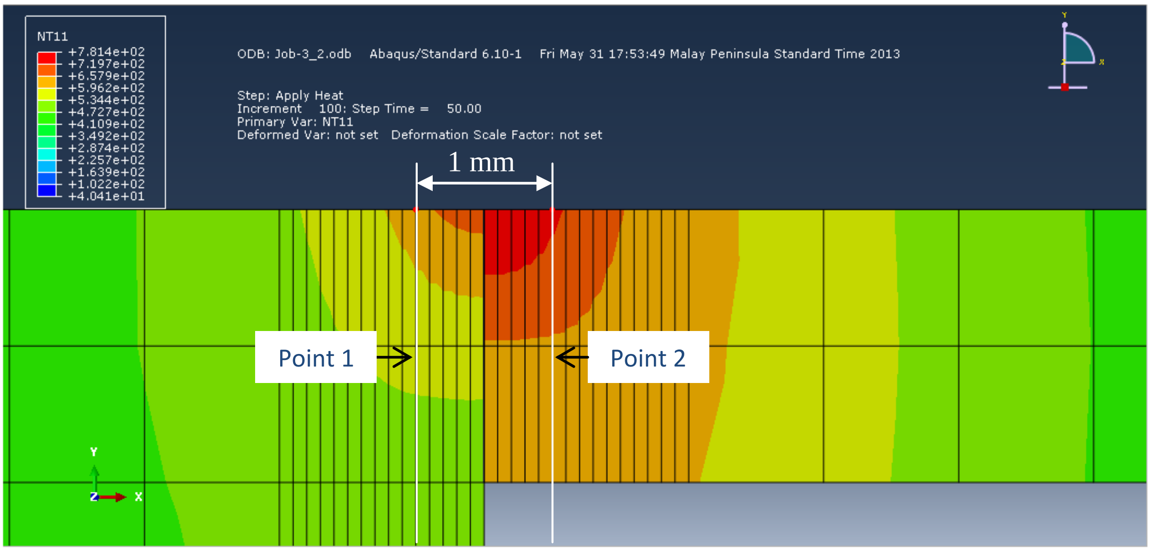

(a) Heating position at 50 % (3 mm) and 50 % (2 mm) with 62 × 10^6 W/m^2 of heat flux

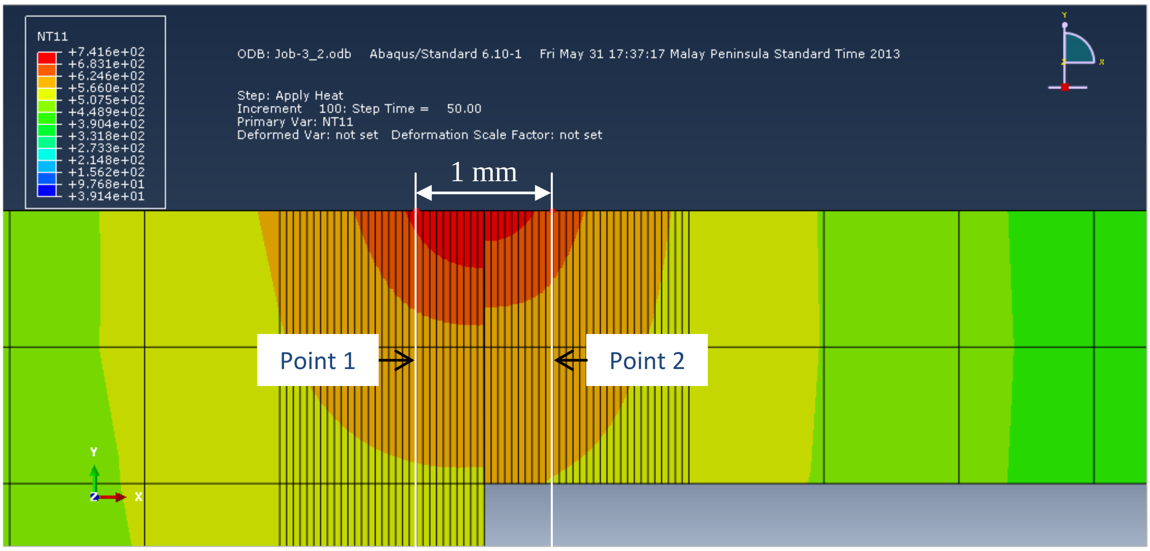

(b) Heating position at 55 % (3 mm) and 45 % (2 mm) with 62 × 10^6 W/m^2 of heat flux

Figure C.2: Different heating position with 62 × 10^6 W/m^2 of heat flux

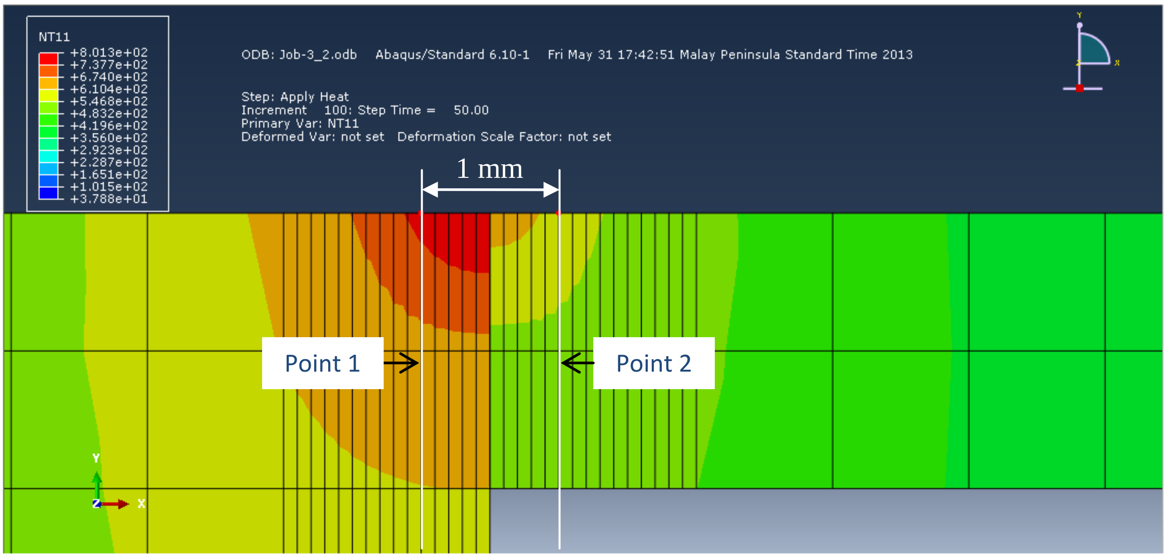

(c) Heating position at 60 % (3 mm) and 40 % (2 mm) with 62 × 10^6 W/m^2 of heat flux

Figure C.2: Continued

APPENDIX C3

PARAMETRIC STUDY ON THICKNESS OF 2 mm AND 1 mm

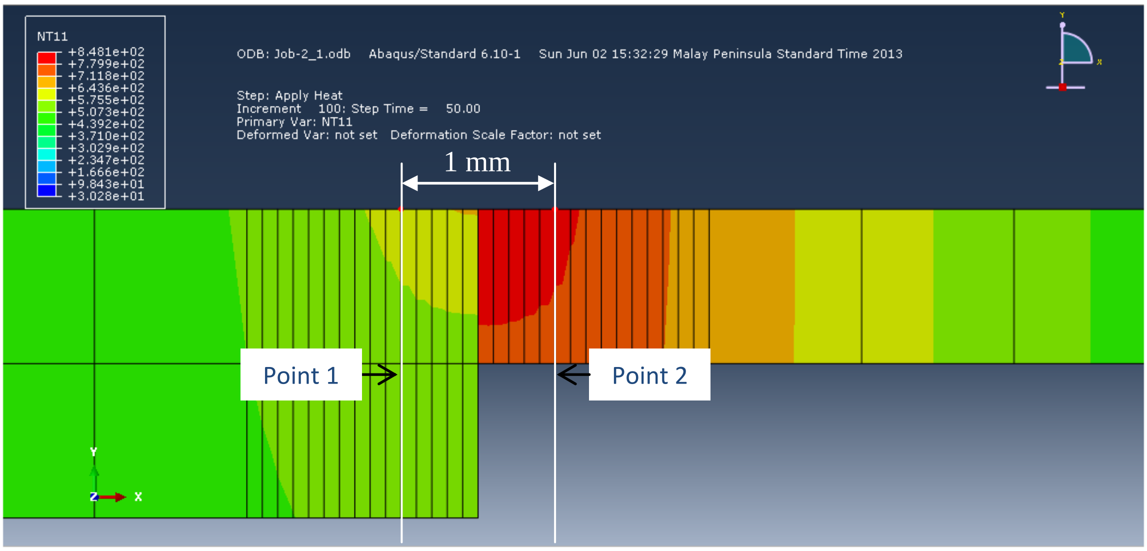

(a) Heating position at 50 % (2 mm) and 50 % (1 mm) with 51×10^6 W/m^2 of heat flux

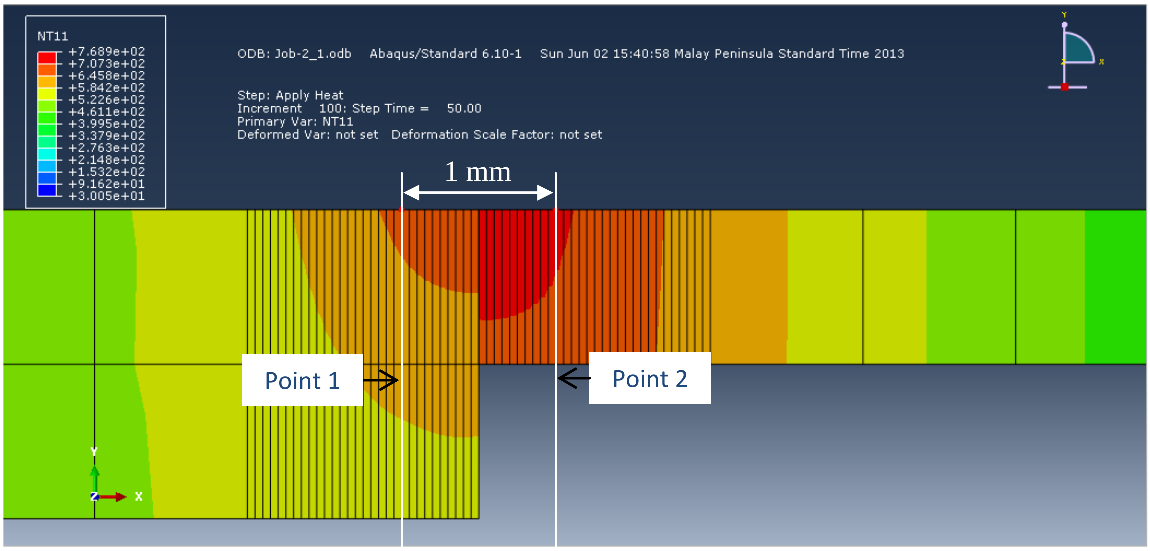

(b) Heating position at 55 % (2 mm) and 45 % (1 mm) with 51×10^6 W/m^2 of heat flux

Figure C.3: Different heating position with 51×10^6 W/m^2 of heat flux

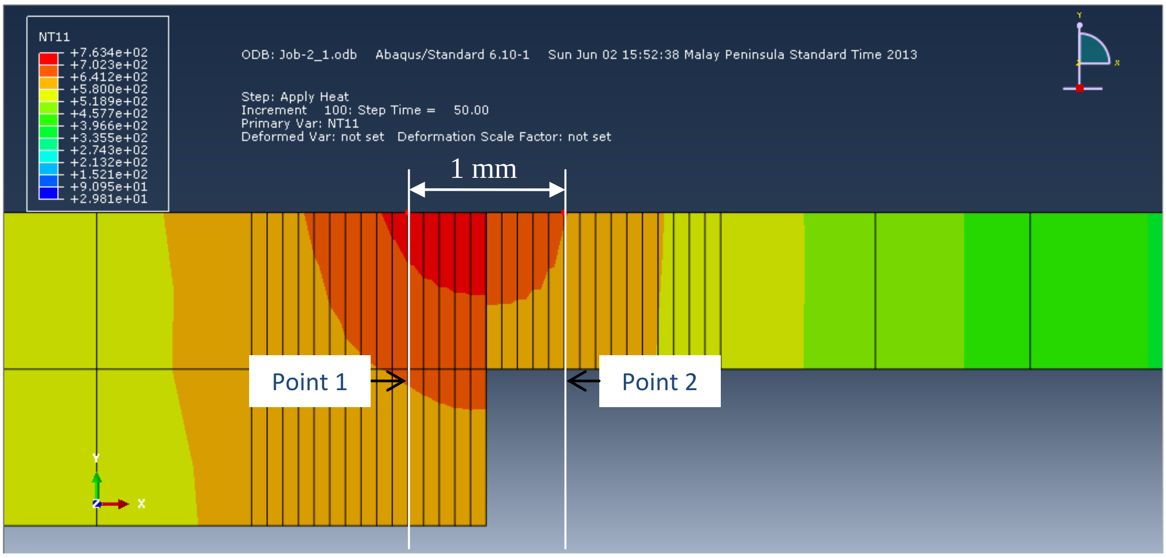

(c) Heating position at 60 % (2 mm) and 40 % (1 mm) with 51 × 10^6 W/m^2 of heat flux

Figure C.3: Continued